

Gaussian Ensemble Belief Propagation for Efficient Inference in High-Dimensional Systems

Dan MacKinlay¹ Russell Tsuchida¹ Dan Pagendam¹ Petra Kuhnert¹

Abstract

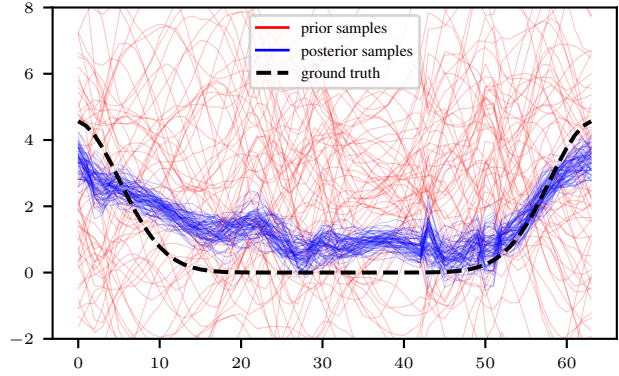
Efficient inference in high-dimensional models remains a central challenge in machine learning. This paper introduces the Gaussian Ensemble Belief Propagation (GEnBP) algorithm, a fusion of the Ensemble Kalman filter and Gaussian Belief Propagation (GaBP) methods. GEnBP updates ensembles by passing low-rank local messages over a graphical model. This combination inherits favourable qualities from each method. Ensemble techniques allow GEnBP to handle high-dimensional states, parameters and intricate, noisy, black-box generation processes. The use of local messages in a graphical model structure ensures that the approach can efficiently handle complex dependence structures. GEnBP is advantageous when the ensemble size may be considerably smaller than the inference dimension. This scenario often arises in fields such as spatiotemporal modelling, image processing and physical model inversion. GEnBP can be applied to general problem structures, including data assimilation, system identification and hierarchical models.

Supporting code is available at github.com/danmackinlay/GEnBP.

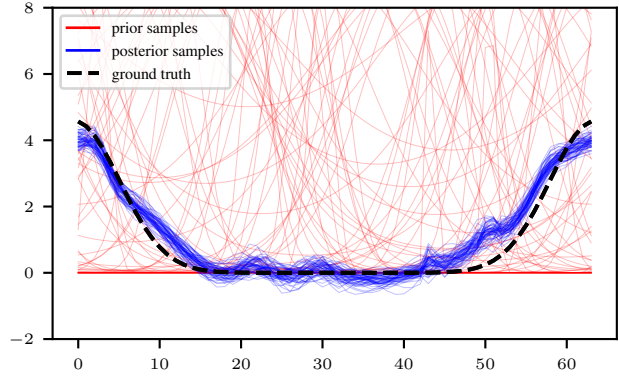
1. Introduction

We combine the Ensemble Kalman filter (EnKF); and Gaussian belief propagation (GaBP), to conduct inference in high-dimensional hierarchical systems.

The EnKF (Evensen, 2003) is a popular method for inference in state space models, operating purely using simulations of the phenomena of interest. A posterior sample of some unobserved state is constructed such that using it as an input to the simulator produces samples from the observation-conditional distribution. Although the state update is justified in terms of a Gaussian approximation to the model based, it avoids constructing the density. This trick is effective in high-dimensional problems, e.g. climate models (Houtekamer & Zhang, 2016) where the normalisation of



(a) GaBP $\widehat{\text{MSE}}=1.93$, $\widehat{\log p}(q|\mathcal{E})=-228$



(b) GEnBP $\widehat{\text{MSE}}=0.167$, $\widehat{\log p}(q|\mathcal{E})=-49.6$

Figure 1: Samples from the prior and posterior for the latent \mathbf{q} for the system identification problem with 1d transport dynamics (sec 4.1). The GEnBP ensemble has size $N=64$, and $N=64$ samples are drawn from the GaBP beliefs.

densities can be expensive. However, the EnKF does not generalise beyond state-filtering.

GaBP (Yedidia et al., 2005) is a specific Gaussian message-passing algorithm for inference in graphical models. Inference is *density-based*, exploiting a nominal joint density over the model state space. This density is approximated by a product of Gaussian factors, which define a graphical model (Koller & Friedman, 2009) over graph \mathcal{G} . Sum-product messages passed along the edges of \mathcal{G} infer some target marginal of interest (Pearl, 2008). GaBP in the mod-

ern sense (Eustice et al., 2006; Ranganathan et al., 2007; Dellaert & Kaess, 2017), uses linear propagation-of-error through the generative model evaluated at its mean to find approximating Gaussian factors for nonlinear relationships. Message-passing approaches are effective in many applications, including Bayesian hierarchical models (Vehtari et al., 2019; Wand, 2017), error correcting codes (Forney, 2001; Kschischang et al., 2001), and Simultaneous Locating and Mapping (SLAM) tasks (Dellaert & Kaess, 2017; Ortiz et al., 2021). Their performance may excel where the variables involved are low-dimensional. However, in high-dimensional cases, the cost of inference is typically prohibitive.

GEnBP borrows strength from both methods, simultaneously attaining the efficiency of the EnKF for high-dimensional data, and GaBP’s ability to handle complex graphical model structures. GEnBP can handle models with noisy and non-linear observation processes, unknown process parameters, and deeply nested hierarchies of dependency between unknown variates, scaling to variables and observations with millions of dimensions. As with both GaBP and EnKF, GEnBP exploits Gaussian approximations, although the statistics are given by empirical samples as in the EnKF rather than by propagation-of-errors as in GaBP. The class of problems amenable to this approach is practically important, encompassing many physical and geospatial systems, including computational fluid dynamics, geophysical model inversion and weather prediction. Such systems generally have a high-dimensional representation, but spatial correlations which induce a low-rank structure well captured by empirical covariance approximations.

1.1. Main Contributions

1. We introduce Gaussian Ensemble Belief Propagation (GEnBP), a method for high-dimensional inference in graphical models with message-passing.
2. GenBP approximates Belief Propagation in Gaussian graphical models using EnKF-like ensemble statistics, rather than linearisation as in traditional GaBP.
3. GEnBP scales to higher dimensions than traditional GaBP, while attaining comparable or superior accuracy in physical problems of practical import
4. GEnBP is enabled by
 - (a) rank-efficient means to propagate high-dimensional Gaussian beliefs, and
 - (b) compute-efficient conversions between Gaussian beliefs and ensemble approximations,

which are to the best of our knowledge novel in this setting.

2. Preliminaries

We introduce the minimum necessary notation and concepts. Deeper background of belief propagation may be found in App. C and of the Ensemble Kalman filter in App. D.

2.1. Models as generative process and as density

The state space of a vector random variate written is bolded, i.e. $\mathbf{x} \in \mathbb{R}^D$, and the corresponding variate itself in sans-serif, \mathbf{x} . We assume that all variates possess densities, so that we may write $\mathbf{x} \sim p(\mathbf{x})$ to assert that \mathbf{x} possesses density p .

The overall model state vector is partitioned into variables related through a structural equation model \mathcal{M} (Wright, 1934), i.e. a list of J generating equations $\{\mathcal{P}_j\}_{1 \leq j \leq J}$,¹

$$\mathcal{P}_j : \mathbb{R}^{D_{\mathcal{I}_j}} \rightarrow \mathbb{R}^{D_{\mathcal{O}_j}} \quad (1)$$

$$\mathbf{x}_{\mathcal{I}_j} \mapsto \mathbf{x}_{\mathcal{O}_j}. \quad (2)$$

Each \mathcal{P}_j induces a relationship between *inputs* \mathcal{I}_j , and *outputs* \mathcal{O}_j .² The *ancestral* variables $\mathcal{A} := \bigcup_{\mathcal{I}_j=\emptyset} \mathcal{O}_j$ are those without inputs. We categorise variables as *Evidence* \mathcal{E} , which will be observed, *latent* \mathcal{L} , which are unobserved, ‘nuisance’ variables, and *query* \mathcal{Q} , whose evidence-conditional distribution is our main interest. In this work, we take the query to be the ancestral variable, $\mathcal{Q} = \mathcal{A}$.³ Our primary target is

$$p(\mathbf{x}_{\mathcal{Q}} | \mathbf{x}_{\mathcal{E}} = \mathbf{x}_{\mathcal{E}}^*) = \frac{\int p(\mathbf{x}_{\mathcal{Q}}, \mathbf{x}_{\mathcal{L}}, \mathbf{x}_{\mathcal{E}} = \mathbf{x}_{\mathcal{E}}^*) d\mathbf{x}_{\mathcal{L}}}{\int p(\mathbf{x}_{\mathcal{Q}}, \mathbf{x}_{\mathcal{L}}, \mathbf{x}_{\mathcal{E}} = \mathbf{x}_{\mathcal{E}}^*) d\mathbf{x}_{\mathcal{Q}} d\mathbf{x}_{\mathcal{L}}}. \quad (3)$$

2.2. BP in graphical models

In graphical models we associate a graph structure \mathcal{G} with the factorisation of the model density and use this to calculate the target distribution (3). Readers unfamiliar with this topic should refer to App. C. We use *loopy belief propagation* (BP) in factor graphs (Kschischang et al., 2001). The factor graph is generated by writing each conditional j as a *factor potential*, f_j ,

$$p(\mathbf{x}) = \prod_j p(\mathbf{x}_{\mathcal{O}_j} | \mathbf{x}_{\mathcal{I}_j}) = \prod_j f_j(\mathbf{x}_{\mathcal{N}_j}). \quad (4)$$

where $\mathcal{N}_j := \mathcal{O}_j \cup \mathcal{I}_j$. The factor graph \mathcal{G} is bipartite, with a factor node j for each factor potential $f_j(\mathbf{x}_{\mathcal{N}_j})$ and a variable node k for each variable \mathbf{x}_k . BP estimates a *belief* over a query node, $b_{\mathcal{G}}(\mathbf{x}_{\mathcal{Q}}) = \int p(\mathbf{x}) d\mathbf{x}_{\setminus \mathcal{Q}}$, by integrating out all other variates.

¹We allow each \mathcal{P} to be a stochastic function, i.e. a deterministic function $\mathbf{x}_{\mathcal{O}_j} = \mathcal{P}_j(\mathbf{x}_{\mathcal{I}_j}, \mathbf{n}_j)$ with unobservable noise term \mathbf{n}_j . We suppress the noise terms for compactness.

²Any of these sets may be empty

³Extending our approach to more general cases is straightforward but complicates the introduction.

Proposition 1 (Belief Propagation on Factor Graphs). *The following messages,*

$$m_{f_j \rightarrow \mathbf{x}_k} = \int \left(f_j(\mathbf{x}_{\mathcal{N}_j}) \prod_{i \in \mathcal{N}_j \setminus k} m_{\mathbf{x}_i \rightarrow f_j} \right) d\mathbf{x}_{\mathcal{N}_j \setminus k} \quad (5)$$

$$m_{\mathbf{x}_k \rightarrow f_j} = \prod_{s \in \mathcal{N}_k \setminus j} m_{f_s \rightarrow \mathbf{x}_k}, \quad (6)$$

iteratively and synchronously propagated between all the nodes in the associated factor graph, yield the approximate marginal at target variable node,

$$b_{\mathcal{G}}(\mathbf{x}_k) = \prod_{s \in \mathcal{N}_k} m_{f_s \rightarrow \mathbf{x}_k} = \int p(\mathbf{x}) d\mathbf{x}_{\setminus k}. \quad (7)$$

The fixed points of this iteration are the fixed points of the Bethe approximation to the target marginal.

Proof. Yedidia et al. (2000). \square

Analysis of quality of this approximation is complicated — see (Yedidia et al., 2005; Weiss & Freeman, 2001) — but in many applications produces SOTA results (Davison & Ortiz, 2019).

2.2.1. THE POSTERIOR GRAPH

We have so far discussed an arbitrary graph \mathcal{G} associated with the generative model; In practice we are not interested in the marginals of this prior graph but of an evidence-conditional posterior graph \mathcal{G}^* which encodes our quantity of interest (3), obtained by conditioning on $\mathbf{x}_{\mathcal{E}} = \mathbf{x}_{\mathcal{E}}^*$. We construct \mathcal{G}^* by altering factors $f_j, \forall j \in \mathcal{N}_{\mathcal{E}}$ in the prior factor graph adjacent to observed variables,

$$f_j(\mathbf{x}_j) \leftarrow f_j^*(\mathbf{x}_{\mathcal{N}_j \setminus \mathcal{E}}) := p(\mathbf{x}_{\mathcal{N}_j \setminus \mathcal{E}} | \mathbf{x}_{\mathcal{E}} = \mathbf{x}_{\mathcal{E}}^*). \quad (8)$$

The target marginal is then $p(\mathbf{x}_{\mathcal{D}} | \mathbf{x}_{\mathcal{E}} = \mathbf{x}_{\mathcal{E}}^*) \approx b_{\mathcal{G}^*}(\mathbf{x}_{\mathcal{D}})$; see Fig 8 in the Appendix..

2.2.2. CONSTRUCTING A NOVEL BP METHOD

To find a target evidence-conditional marginal $b_{\mathcal{G}^*}(\mathbf{x}_{\mathcal{D}})$ from a prior factor graph we need to be able to 1) find posterior factors by conditioning (8), and 2) calculate the BP messages of Prop. 1. A sufficient set of operations defined upon factor and variable densities is as follows.

Definition 1. *Consider the state space $\mathbf{x} = \begin{bmatrix} \mathbf{x}_k \\ \mathbf{x}_{\ell} \end{bmatrix}$ at some node in a factor graph, with parametric density $f(\mathbf{x}; \boldsymbol{\theta})$. The sufficient operations for BP are:*

Conditioning:

$$f(\mathbf{x}; \boldsymbol{\theta}), \mathbf{x}_k^* \mapsto f^*(\mathbf{x}_{\ell}; \boldsymbol{\theta}_{\ell}^*) =: f(\mathbf{x}_{\ell} | \mathbf{x}_k = \mathbf{x}_k^*); \quad (9)$$

Marginalisation:

$$f(\mathbf{x}; \boldsymbol{\theta}) \mapsto f(\mathbf{x}_k; \boldsymbol{\theta}_k) =: \int f(\mathbf{x}; \boldsymbol{\theta}) d\mathbf{x}_{\ell}; \quad (10)$$

Multiplication:

$$f(\mathbf{x}; \boldsymbol{\theta}), f(\mathbf{x}_k; \boldsymbol{\theta}_k) \mapsto f(\mathbf{x}; \boldsymbol{\theta}') =: f(\mathbf{x}; \boldsymbol{\theta}) f(\mathbf{x}_k; \boldsymbol{\theta}_k). \quad (11)$$

Typically such operations are implemented in terms of the $\boldsymbol{\theta}_{(\cdot)}$ parameters of the density functions.

Remark 1. *To calculate the marginal belief over a target variable $\mathbf{x}_{\mathcal{D}}$ by message passing in a observation-conditional factor graph (8) a sufficient set of operations defined over factors and variables is (9), (10) and (11).*

2.2.3. GAUSSIAN DISTRIBUTIONS IN BP

BP is tractable in the case that all factors are Gaussian (Yedidia et al., 2000), a fact exploited in classic GaBP (Dellaert & Kaess, 2017), which we introduce here. If the relationships between variables are linear with additive Gaussian noise and the ancestral distributions are Gaussian then the potential over each factor is Gaussian. Then, all of the requisite operations of Rem. 1 have closed form (Bickson, 2009). We use two forms for the Gaussian density. The *moments-form* Gaussian density is

$$\phi_M(\mathbf{x}; \mathbf{m}, K) = |2\pi K|^{-1/2} e^{-1/2(\mathbf{x}-\mathbf{m})^{\top} K^{-1}(\mathbf{x}-\mathbf{m})} \quad (12)$$

The *canonical form*

$$\phi_C(\mathbf{x}; \mathbf{n}, P) = |P/2\pi|^{1/2} e^{-\frac{\mathbf{x}^{\top} P \mathbf{x} + \mathbf{n}^{\top} \mathbf{x} - \frac{\mathbf{n}^{\top} P^{-1} \mathbf{n}}{2}}{2}}, \quad (13)$$

The respective parameters are with mean \mathbf{m} and covariance K ; and precision $P = K^{-1}$ and information $\mathbf{n} = P\mathbf{m}$, assuming the necessary inverses exist. See Appendix C.3 for details. The most challenging operation is multiplication (11), which forms a major part of this paper,

$$\phi_C(\mathbf{x}; \mathbf{n}, P) \phi_C(\mathbf{x}_k; \mathbf{n}', P') \propto \phi_C(\mathbf{x}; \mathbf{n} + \mathbf{n}', P + P'). \quad (14)$$

In practice, GaBP is frequently applied where the factor potentials arise from some nonlinear simulator \mathcal{P} , and the joint covariance may not be actually Gaussian. Standard practice (e.g. Ranganathan et al., 2007) is to use propagation-of-errors to find approximating densities to the target. Introducing Jacobian at the mean $\mathbf{J} = \nabla_{\mathbf{x}} \mathcal{P}(\mathbf{x})|_{\mathbf{x}=\mathbf{m}_1}$, the bivariate case where $\mathbf{x}_2 = \mathcal{P}(\mathbf{x}_1)$, $\mathbb{E}[\mathbf{x}_1] = \mathbf{m}_1$ and $\text{Var} \mathbf{x}_1 = K_1$,

$$\begin{bmatrix} \mathbf{x}_1 \\ \mathbf{x}_2 \end{bmatrix} \overset{\text{approx}}{\sim} \phi_M \left(\begin{bmatrix} \mathbf{x}_1 \\ \mathbf{x}_2 \end{bmatrix}; \begin{bmatrix} \mathbf{m}_1 \\ \mathcal{P}(\mathbf{m}_1) \end{bmatrix}, K \right) \text{ where} \quad (15)$$

$$K = \begin{bmatrix} K_1 & \mathbf{J}K_1 \\ K_1 \mathbf{J}^{\top} & \mathbf{J}K_1 \mathbf{J}^{\top} \end{bmatrix}. \quad (16)$$

GaBP scales unfavourably with the dimension of nodes, paying memory cost $\mathcal{O}(D^2)$ and compute cost $\mathcal{O}(D^3)$ whenever a $D \times D$ covariance matrix is inverted.

2.3. Ensemble Kalman Filtering

A method which ameliorates large- D difficulties is EnKF. Where the GaBP method summarises inference in terms of the parameters of a Gaussian distribution, the EnKF summarises the joint distribution in terms of an *ensemble* of Monte Carlo samples, i.e. a matrix of N samples, $X := [\mathbf{x}^{(n)}]_{1 \leq n \leq N}$ drawn i.i.d. from the prior distribution, $\mathbf{x}^{(n)} \sim \phi_M(\mathbf{x}; \mathbf{m}, K)$. Introducing the matrices $A_N := [\frac{1}{N} \ \cdots \ \frac{1}{N}]^\top$, $B_N := [1 \ \cdots \ 1]$ and $C_N := I_N - A_N B_N$, we define

$$\bar{X} := X A_N \quad \text{Ensemble mean} \quad (17)$$

$$\check{X} := X - X A_N B_N = X C_N. \quad \text{Ensemble deviation} \quad (18)$$

We hereafter suppress N , which is uniquely determined by context. Overloading the mean and variance operations to describe empirical moment of ensembles, we write

$$\widehat{\mathbb{E}}X = \bar{X} \quad (19)$$

$$\widehat{\text{Var}}_V X = \frac{1}{N-1} \check{X} \check{X}^\top + V \quad (20)$$

$$\widehat{\text{Cov}}(X, Y) = \frac{1}{N-1} \check{X} \check{Y}^\top \quad (21)$$

V is a diagonal matrix *nugget* term, typically set to $\sigma^2 I$. Setting $\sigma > 0$ is useful for numerical stability, and to encode model uncertainty. Such diagonal terms are in practice algorithm hyperparameters, and also arise in GaBP.

The statistics of ensemble X define an implied Gaussian density, $\mathbf{x} \sim \phi_M(\mathbf{x}; \bar{X}, \widehat{\text{Var}}_V X)$. The prior model ensembles are sampled by ancestral sampling with generative equations (31).

Two of the BP operations from Rem. 1 are known for the EnKF.

Proposition 2. Partition $\mathbf{x} = \begin{bmatrix} \mathbf{x}_k \\ \mathbf{x}_\ell \end{bmatrix}$ so $X = \begin{bmatrix} X_k \\ X_\ell \end{bmatrix}$, and

$$X \sim \phi_M \left(\begin{bmatrix} \mathbf{x}_k \\ \mathbf{x}_\ell \end{bmatrix}; \begin{bmatrix} \bar{X}_k \\ \bar{X}_\ell \end{bmatrix}, \begin{bmatrix} \widehat{\text{Var}}_V X_k & \widehat{\text{Cov}}(X_\ell, X_k) \\ \widehat{\text{Cov}}(X_k, X_\ell) & \widehat{\text{Var}}_V(X_\ell) \end{bmatrix} \right). \quad (22)$$

In ensemble form, conditioning (9) becomes

$$X, \mathbf{x}_k^* \mapsto X_\ell + \widehat{\text{Cov}}(X_\ell, X_k) \widehat{\text{Var}}_V^{-1}(X_k) (\mathbf{x}_k^* B - X_k) \quad (23)$$

The time cost of (23) is $\mathcal{O}(N^3 + N^2 D_{\mathbf{x}_k})$. Marginalisation (10) is simply truncation, $X \mapsto X_k$.

Proof. Appendix D. \square

Whether the EnKF is a good approximation to the target distribution for any N depends on the specific model but

in many spatiotemporal systems we find good results for $N \ll D$, in which case the cost conditioning is superior to the $\mathcal{O}(D_{\mathbf{x}_k}^3)$ cost of the GaBP.

The full EnKF algorithm iteratively applies this conditional update by exploiting the state-space model structure, but does not generalise to other model structures since it does not define the density-multiplication operation (11) needed for belief propagation over arbitrary graphs. In the sequel, we explore how to effectively combine the strengths of EnKF and GaBP.

3. Gaussian Ensemble Belief Propagation

We introduce GEnBP, an algorithm that interleaves EnKF- and GaBP-type operations. The GEnBP is related to GaBP in the same way that the Ensemble Kalman Filter is related to the Extended Kalman Filter: both extend a method originally developed under linear assumptions to address more complex, non-linear scenarios. Both use Gaussian approximations, albeit in different ways, to approximate the true posterior distribution; GEnBP uses ensemble statistics, while GaBP uses propagation-of-errors.

Throughout we regard an approximation $\phi_M(\hat{\mathbf{m}}, \hat{K})$ to a target Gaussian $\phi_M(\mathbf{m}, K)$ to be the *best* if $\hat{\mathbf{m}} = \mathbf{m}$ and Frobenius loss $\|\hat{K} - K\|_F$ is minimised. Statistically, this equates to minimising the Maximum Mean Discrepancy between the two distributions with respect to the polynomial kernel of order 2 (Sriperumbudur et al., 2010, Example 3).

GEnBP samples from the generative prior, converts the ensemble statistics to canonical form, conducts belief propagation, and then recovers ensemble samples matching the updated beliefs (Tab. 1, Alg. 1). Although there are many steps in the algorithm, the shared core strategy is constructing all the steps of a Belief propagation-type algorithm using low-rank Gaussian statistics from the EnKF approximation without ever forming a full covariance matrix.

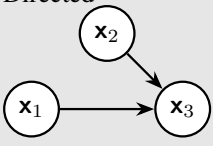
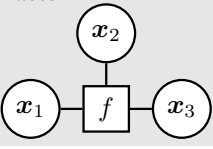
3.1. Nearly-low-rank Gaussian parameters

The GEnBP workhorse is efficient computation using the *nearly-low-rank* Gaussian moments induced by the ensemble samples. This enables translation between ensemble statistics, various parameterisations, and efficient operations upon those parameters.

Definition 2. A positive-definite, symmetric matrix $K \in \mathbb{R}^{D \times D}$ is nearly-low-rank if $K = V \pm LL^\top$ where $L \in \mathbb{R}^{D \times N}$ is a low rank component matrix with $N \ll D$ by assumption and $V = \text{diag}(\mathbf{v})$ is a $D \times D$ diagonal matrix.

The empirical variance we use in the EnKF (20) has such a nearly-low-rank structure with component $L = \frac{1}{\sqrt{N-1}} \check{X}$ and diagonal $V = \sigma^2 I$. Properties of such matrices are expanded in App. F. We initialise the belief-propagation

Table 1: Relations in Gaussian Ensemble Belief Propagation

	Generative	Density-based
Operations	<ul style="list-style-type: none"> • Sample • Condition 	<ul style="list-style-type: none"> • Propagate
Graph type	Directed 	Factor 
Decomposition	$\mathbf{x}_3 = \mathcal{P}(\mathbf{x}_1, \mathbf{x}_2)$	$f(x_1, x_2, x_3)$
Node Parameters	Empirical moments \mathbf{m}, \mathbf{K}	Canonical parameters \mathbf{n}, \mathbf{P}

Empirical statistics
 Ensemble recovery

Algorithm 1 GENBP

Require: Graph \mathcal{G} , set of generative processes $\{\mathcal{P}_j\}_j$, observations $\mathbf{x}_{\mathcal{O}}$, ancestral sample $X_{\mathcal{A}}$.

Ensure: Observation-conditional sample $X_{\mathcal{O}}^*$.

- 1: **while** not converged **do**
- 2: Sample ensemble from the generative processes \mathcal{P}_j on \mathcal{G} using (4)
- 3: Convert \mathcal{G} into the conditional graph \mathcal{G}^* by conditioning observed factors (8) using (23)
- 4: Convert variables and factors to nearly-low-rank canonical form {Sec. 3.1}
- 5: Propagate nearly-low-rank messages on \mathcal{G}^* {Sec. 3.3/Alg. 2}
- 6: Conform ancestral nodes to belief $T(X_{\mathcal{O}}^*) \sim b_{\mathcal{G}^*}(\mathbf{x}_{\mathcal{A}})$ {Sec. 3.4}
- 7: **end while**
- 8: Return Approximate posterior sample $X_{\mathcal{O}}^*$.

stage of the algorithm (step 1), setting the distribution for each factor f_j^* to the empirical distribution of the ensemble at that factor, X_j ,

$$f_j^* \sim \phi_M(\mathbf{x}; \bar{X}_j, \widehat{\text{Var}}_{\gamma^2 I} X). \quad (24)$$

Proposition 3. Suppose $\mathbf{x} \sim \phi_M(\cdot; \mathbf{m}, \mathbf{K})$ has nearly-low-rank variance $\mathbf{K} = \mathbf{L}\mathbf{L}^\top + \mathbf{V}$, $\mathbf{L} \in \mathbb{R}^{D \times N}$. We may find the parameters of that density in canonical form $\phi_C(\cdot; \mathbf{n}, \mathbf{P})$ as $\mathbf{n} = \mathbf{P}\mathbf{m}$ and precision $\mathbf{P} = \mathbf{K}^{-1} = \mathbf{U} - \mathbf{R}\mathbf{R}^\top$, at a time cost of $\mathcal{O}(N^3 + N^2D)$. Further, we may recover the moments-form from the canonical at the same cost.

Proof. Appendix F.3 □

3.2. Nearly-low-rank belief propagation

Density multiplication (14) is simple in the nearly-low-rank representation.

Proposition 4. Suppose we are given two canonical-form Gaussian densities with respective information and precisions \mathbf{n}', \mathbf{P}' and $\mathbf{n}'', \mathbf{P}''$, where the precisions are both nearly low rank, $\mathbf{P}' = \mathbf{U}' - \mathbf{R}'\mathbf{R}'^\top$ and $\mathbf{P}'' = \mathbf{U}'' - \mathbf{R}''\mathbf{R}''^\top$ where $\mathbf{R}' \in \mathbb{R}^{D \times N'}$ and $\mathbf{R}'' \in \mathbb{R}^{D \times N''}$ and $\mathbf{U}', \mathbf{U}''$ diagonal. Then the parameters \mathbf{n}, \mathbf{P} of the multiplied density $\phi_C(\cdot, \mathbf{n}, \mathbf{P}) = \phi_C(\cdot, \mathbf{n}', \mathbf{P}')\phi_C(\cdot, \mathbf{n}'', \mathbf{P}'')$ are given by

$$\mathbf{n} = \mathbf{n}' + \mathbf{n}'' \text{ and} \quad (25)$$

$$\mathbf{P} = \mathbf{P}' + \mathbf{P}'' = \mathbf{U} - \mathbf{R}\mathbf{R}^\top, \text{ where} \quad (26)$$

$$\mathbf{U} = \mathbf{U}' + \mathbf{U}'', \text{ and } \mathbf{R} = [\mathbf{R}' \quad \mathbf{R}''] \quad (27)$$

\mathbf{P} is also nearly-low-rank, with $\mathbf{R} \in \mathbb{R}^{D \times (N' + N'')}$.

Proof. Follows from (44) and (73) in the appendix. □

3.3. GENBP messages

The most complicated step is the factor-to-variable message (5), $f_j \rightarrow \mathbf{x}_k$, which is detailed in Alg. 2 for a single incoming message $\mathbf{x}_\ell \rightarrow f_j$. Generalisation to multiple incoming messages is by iterative application of the algorithm. Variable-to-factor messages are a degenerate case.

This step is the most costly. Suppose we wish to calculate an outgoing message from D -dimensional factor f , with K neighbours, to a d -dimensional variable node \mathbf{x} . In the worst case, messages are incoming from $K - 1$ neighbours, so the concatenated components of the factor belief precision matrix in step 2 is a $D \times NK$ matrix. Inverting this (step 2) costs $\mathcal{O}(DN^2K^2 + N^3K^3)$ (Prop 8). We

Algorithm 2 GEnBP $f_j \rightarrow \mathbf{x}_k$ factor-to-variable message with a single incoming message $\mathbf{x}_\ell \rightarrow f_j$.

Require: Gaussian factor canonical parameters for f_j , $\mathbf{n} = \begin{bmatrix} \mathbf{n}_\ell \\ \mathbf{n}_k \end{bmatrix}$, $\mathbf{P} = \mathbf{U} - \begin{bmatrix} \mathbf{R}_\ell \\ \mathbf{R}_k \end{bmatrix} \begin{bmatrix} \mathbf{R}_\ell \\ \mathbf{R}_k \end{bmatrix}^\top$ for $\mathbf{U} = \text{diag} \left(\begin{bmatrix} \mathbf{u}_\ell \\ \mathbf{u}_k \end{bmatrix} \right)$ with $\mathbf{R}_\ell \in \mathbb{R}^{D_\ell \times N}$, $\mathbf{R}_k \in \mathbb{R}^{D_k \times N}$

Require: $\mathbf{x}_k \rightarrow f_j$ Gaussian message parameters $\mathbf{n}'_k \in \mathbb{R}^{D_k}$ and precision $\mathbf{P}_k = \mathbf{U}'_k - \mathbf{R}'_k \mathbf{R}'_k{}^\top$ with $\mathbf{R}'_k \in \mathbb{R}^{D_k \times N'}$ and $\mathbf{U}'_k = \text{diag}(\mathbf{u}'_k)$

Ensure: $f_j \rightarrow \mathbf{x}_\ell$ Gaussian message parameters \mathbf{n}'_ℓ , $\mathbf{P}'_\ell = \mathbf{U}'_\ell - \mathbf{R}'_\ell \mathbf{R}'_\ell{}^\top$

- 1: Form joint information vector $\mathbf{n}_{\text{prod}} = \begin{bmatrix} \mathbf{n}_\ell \\ \mathbf{n}_k + \mathbf{n}'_k \end{bmatrix}$.
- 2: Form joint precision $\mathbf{P}_{\text{prod}} = \mathbf{U}_{\text{prod}} - \mathbf{R}_{\text{prod}} \mathbf{R}_{\text{prod}}^\top$, $\mathbf{R}_{\text{prod}} = \begin{bmatrix} \mathbf{R}_\ell & \mathbf{0} \\ \mathbf{R}_k & \mathbf{R}'_k \end{bmatrix}$ and $\mathbf{U}_{\text{prod}} = \text{diag} \left(\begin{bmatrix} \mathbf{u}_\ell \\ \mathbf{u}_k + \mathbf{u}'_k \end{bmatrix} \right)$
- 3: Form joint covariance $\mathbf{K}_{\text{prod}} = \mathbf{P}_{\text{prod}}^{-1} = \mathbf{V}_{\text{prod}} + \mathbf{L}_{\text{prod}} \mathbf{L}_{\text{prod}}^\top$ where $\mathbf{L}_{\text{prod}} \in \mathbb{R}^{(D_k + D_\ell) \times (N + N')}$ and $\mathbf{V} = \text{diag}(\mathbf{v}_{\text{prod}})$
- 4: Calculate joint mean $\mathbf{m}_{\text{prod}} = \mathbf{P}_{\text{prod}} \mathbf{n}_{\text{prod}}$
- 5: Form the marginal mean over \mathbf{x}_ℓ , $\mathbf{m}_\ell = \mathbf{m}_{\text{prod}}[1 : D_k]$
- 6: Form the marginal covariance over \mathbf{x}_ℓ , $\mathbf{K}_\ell = \mathbf{V}_\ell + \mathbf{L}_\ell \mathbf{L}_\ell^\top$ where $\mathbf{L}_{\text{prod}}[1 : D_k, 1 : (N' + N)]$, $\mathbf{V}_\ell = \text{diag}(\mathbf{v}_{\text{prod}}[1 : D_k])$
- 7: Constrain the rank of $\mathbf{K}_\ell \leftarrow \mathbf{K}'_\ell = \mathbf{V}_\ell + \mathbf{L}'_\ell \mathbf{L}'_\ell{}^\top$ to N setting $\mathbf{L}'_\ell = \mathbf{A}\mathbf{S}$ for \mathbf{A} the left singular vectors and \mathbf{S} the top n singular values
- 8: Calculate the marginal precision $\mathbf{P}'_\ell = \mathbf{K}'_\ell^{-1} = \mathbf{U}_\ell - \mathbf{R}_\ell \mathbf{R}_\ell{}^\top$
- 9: Calculate the marginal information vector $\mathbf{n}'_\ell = \mathbf{P}'_\ell \mathbf{m}_\ell$
- 10: Return canonical information vector \mathbf{n}'_ℓ
- 11: Return canonical precision \mathbf{P}'_ℓ

discover the size- N basis using SVD via F.5 at a cost of $\mathcal{O}(DNK \log N + N^2(D + NK))$. Marginalising by truncating to the d dimensions spanned by the variable node yields $d \times N$ variance component matrices. The canonical form of the reduced-rank belief may be found with time cost of $\mathcal{O}(N^3 + N^2d)$ using 9, at an overall cost of $\mathcal{O}(DN^2K^2 + N^3K^3)$.

3.4. Nearly-low-rank ensemble conformation

The final step of the GEnBP algorithm is *ensemble conformation*, which transforms a prior ensemble into a posterior ensemble whose statistics are maximally consistent with the posterior belief $b_{\mathcal{G}^*}(\mathbf{x}_{\mathcal{Q}}) = \phi_M(\mathbf{x}_{\mathcal{Q}}; \mathbf{m}_{\mathcal{Q}}, \mathbf{K}_{\mathcal{Q}})$ at query node \mathcal{Q} , i.e. $T(X) \stackrel{\text{approx}}{\sim} b_{\mathcal{G}^*}$. We suppress the \mathcal{Q} subscript hereafter. Restricting ourselves to affine transformations $T_{\mu, \mathbf{T}} : X \mapsto \mu \mathbf{B} + \check{\mathbf{X}} \mathbf{T}$ leaves the parameters $\mu \in \mathbb{R}^D$, $\mathbf{T} \in \mathbb{R}^{M \times M}$ to be chosen. Fixing $\mu \equiv \mathbf{m}$, we choose \mathbf{T} to optimise the Frobenius distance

between the variances of the mapped ensemble and the target $\mathbf{K} = \mathbf{L}\mathbf{L}^\top + \mathbf{V}$, with \mathbf{V} diagonal,

$$\mathbf{T} := \text{argmin}_{\mathbf{T}^*} \left\| \widehat{\text{Var}}_{\eta^2 \mathbf{I}}(\mu \mathbf{B} + \check{\mathbf{X}} \mathbf{T}^*) - \mathbf{K} \right\|_F^2 \quad (28)$$

\mathbf{T} is identifiable only up to a unitary transform. We therefore find $\mathbf{M} := \mathbf{T}\mathbf{T}^\top$ from the space of positive definite matrices, selecting a \mathbf{T} from \mathbf{M} by factorisation.

Proposition 5. Any symmetric positive semi-definite matrix $\mathbf{M} = \mathbf{T}\mathbf{T}^\top$ which satisfies

$$\check{\mathbf{X}}^\top \check{\mathbf{X}} \mathbf{M} \check{\mathbf{X}}^\top \check{\mathbf{X}} = (N-1) \left(\check{\mathbf{X}}^\top \mathbf{L} (\check{\mathbf{X}}^\top \mathbf{L})^\top - \check{\mathbf{X}}^\top (\mathbf{V} - \eta^2 \mathbf{I}) \check{\mathbf{X}} \right).$$

defines an affine transform which minimises (28). Such an \mathbf{M} may be found with memory complexity $\mathcal{O}(M^2 + N^2)$ and time complexity $\mathcal{O}(N^3 + DN^2 + DM^2)$ without forming $\mathbf{K} \in \mathbb{R}^{D \times D}$.

Proof. Appendix H □

For a variable with K neighbours, the worse-case is $M = KN$ so the cost comes to $\mathcal{O}(N^3 + DN^2K^2)$. The cost of finding the target covariance from the belief precision is $\mathcal{O}(M^3 + DM^2) = \mathcal{O}(K^3N^3 + DK^2N^2)$ by (79), so our total cost for ensemble recovery is $\mathcal{O}(K^3N^3 + DN^2K^2)$.

3.5. Total computational cost

Analysis of the computational cost of the GEnBP algorithm depends upon graph structure and the various tuning parameters. The size of the ensemble in GEnBP is a free parameter controlling the fidelity of the approximation to classical GaBP, and also the computational cost. Empirically, in many useful problems $N \ll D$ (App. B.2). Detailed costs are collated in Tab. 2 in App. I. GEnBP is favourable for all operations for a fixed factor degree K .

Care is needed in interpreting costs involving the node degree K . We can reduce the size of large factor nodes by decomposing them into a chain nodes with lower degree, the *Forney* factorisation (Forney, 2001). This modification controls K without altering models' marginal distributions (de Vries & Friston, 2017). In the system identification experiment, K may be large, since the latent parameter influences every timestep so has many neighbours, but the Forney representation caps $K \leq 4$. The net impact depends upon the graphical structure, but in these experiments, the cost of the additional messages is outweighed by the reduction in the cost of the messages.

4. Experiments

We compared GEnBP against GaBP in two synthetic randomised benchmarks. In both, the graph structure is a system identification task (Appendix A.1), where a static parameter of interest influences a noisily observed, nonlinear

dynamical system. For $t = 1, 2, \dots, T$ we define

$$\mathbf{x}_t = \mathcal{P}_x(\mathbf{x}_{t-1}, \mathbf{q}), \quad \mathbf{y}_t = \mathcal{P}_y(\mathbf{x}_t) \quad (29)$$

where evidence is $\mathcal{E} = \{\mathbf{y}_t = \mathbf{y}_t^*\}_{1 \leq t \leq T}$ and the query is $\mathcal{Q} = \mathbf{q}$.⁴

The GaBP implementation is that of Ortiz et al. (2021), extended to allow an arbitrary prior covariance. Hyperparameters and specifications of the model are not directly comparable between the methods. We ameliorate this by choosing favourable values for each algorithm. We measure performance by mean squared error (MSE) of the posterior mean estimate $\mathbb{E}b_{\mathcal{G}^*}(\mathbf{q}) - q_0$ and the log-likelihood $\log b_{\mathcal{G}^*}(q_0; \mathbf{q})$ at ground truth q_0 . Additional experiments and details are in App B.

4.1. 1d transport model

The *transport* problem is a simple, 1d nonlinear dynamical system chosen for ease of visualisation(Appendix A.2). States are subject to both transport and diffusion, where the transport term introduces nonlinearity. Observations are subsampled state vectors perturbed by additive Gaussian noise. Fig. 1 shows samples from the prior and posterior distributions for each model. In this system, GEnBP estimate is substantially more accurate in terms of both posterior likelihood and MSE, as can be seen in the tighter clustering of the posterior samples about ground-truth.

4.2. 2d fluid dynamics model

In the computational fluid dynamics (CFD) problem (Appendix A.3), the states are governed by discretised Navier-Stokes equations over a 2d spatial domain. The parameter of interest is a static latent forcing field \mathbf{q} . Each $d \times d$ discretised state is stacked into a vector $\mathbf{x} \in \mathbb{R}^{d^2}$. In our 2d incompressible equations the state field and forcing fields are scalar, so $D_{\mathcal{Q}} = D_{\mathbf{x}_t} = d^2$.

Fig 2 demonstrates that GEnBP solving the target with a comparable accuracy and posterior likelihood but scales to a far higher dimension than GaBP. GEnBP is strictly dominant in higher dimension, in terms of MSE, likelihood and compute cost. Note the GaBP experiments are truncated because experiments with dimension $D_{\mathcal{Q}} > 1024$ failed to complete due to resource exhaustion. We caution against interpreting the run time of the algorithm too literally. The high-dimensional jacobian calculation in the GaBP algorithm is not parallelised effectively by the Pytorch library, which penalises that algorithm. On the other hand, optimal calculation of high-dimensional jacobian matrices is difficult, scaling in the worst case as $\mathcal{O}(D)$ (Margossian, 2019), so avoiding them in the GEnBP algorithm maybe

⁴If \mathbf{q} were known, estimating $\{\mathbf{x}_t\}_t$ from $\{\mathbf{y}_t\}_t$ would be a filtering problem, soluble by EnKF.

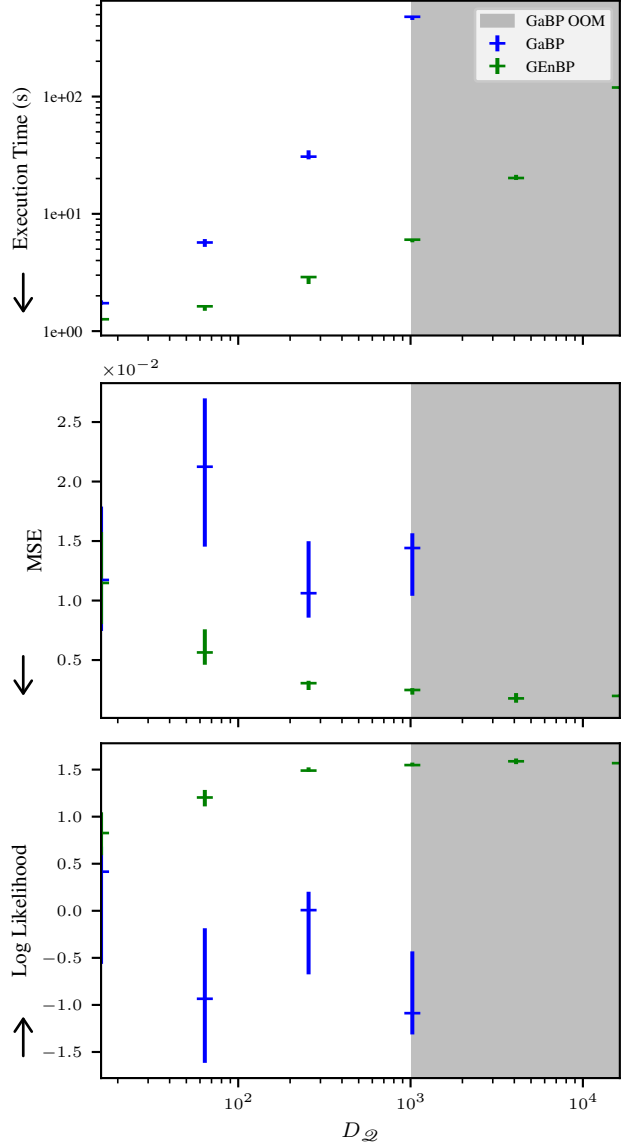


Figure 2: Influence of dimension $D_{\mathcal{Q}}$. Error bars show empirical 50% intervals from $n = 10$ independent runs.

be an advantage to the practitioner both in speed and in implementation burden.

Fig 3 show the effect of the viscosity parameter ν as it varies from laminar to turbulent flow regimes, producing diverse nonlinear behaviours (See Fig. 5 for example simulations). GEnBP still strictly dominates GaBP in terms of time. It generally dominates in MSE, although there are parameter ranges where the performance is indistinguishable or slightly worse. With regards to posterior log-likelihood of the ground-truth, GEnBP is dominant in the low viscosity (turbulent) regime. In the high viscosity (laminar flow) regime, GaBP has the advantage by this metric.

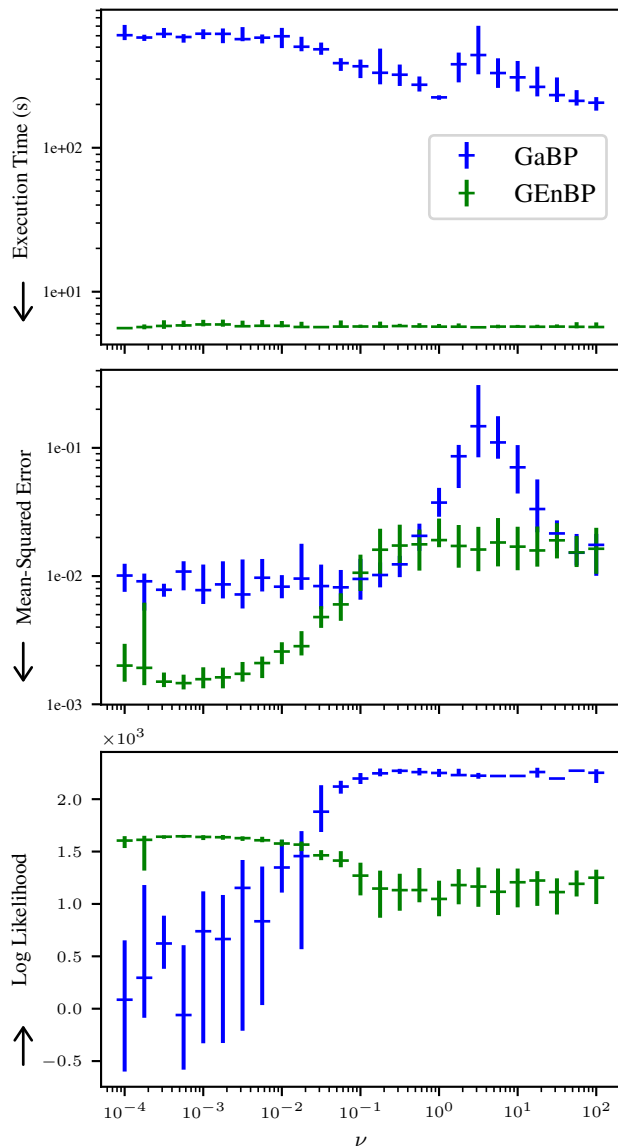


Figure 3: Influence of viscosity ν on inference. Error bars show empirical 50% intervals from $n = 40$ independent runs.

5. Conclusions

GEnBP advances the frontier of possible problems that can be solved using probabilistic graphical models. It scales to higher factor dimension than traditional GaBP, achieving in practice superior accuracy for some problems of interest. By employing ensemble approximations, GEnBP can accommodate larger and more complex factors, important in a broad range of real-world problems. Unlike EnKF, which would be traditionally used for high dimensional systems, GEnBP can handle intricate dependencies and not just state filtering. It does not need gradients, and yet frequently surpasses the performance of GaBP, which does.

There are some limitations. First, GEnBP introduces additional tuning parameters, which require careful adjustment. Second, GEnBP requires an increased number of model executions in the sampling stage, although we note that the cost of high dimensional jacobian calculations, as used in GaBP, can in practice be worse. As with EnKF, we can generally only expect GEnBP to be effective in systems where the underlying dynamics are nearly-low rank, i.e. where the system can be well-approximated by some low-dimensional subspace. Finally, just as the GaBP and EnKF, GEnBP still ultimately exploits Gaussian approximations and thus is also constrained to unimodal distributions. Despite these limitations, its scalability and flexibility makes it a promising tool for a broad range of applications, notably geospatial predictions.

We note that both the GaBP and EnKF literatures contain many additional improvements that we look forward to integrating into GEnBP in further research, e.g. graph pruning for improved computational efficiency (Eustice et al., 2006) or handling outliers using robust distributions (Agarwal et al., 2013). There are also many other generalisations of GaBP, such as particle- (Ihler & McAllester, 2009) or Stein- (Zhuo et al., 2018) message-passing algorithms, whose connection remains to be explored.

This work has no known wider negative societal implications other than the standard consequences of improved generic inference.

6. Acknowledgements

We are indebted to Laurence Davies and Hadi Afshar for helpful discussions and feedback on this work.

References

- Agarwal, P., Tipaldi, G. D., Spinello, L., Stachniss, C., and Burgard, W. Robust map optimization using dynamic covariance scaling. In *2013 IEEE International Conference on Robotics and Automation*, pp. 62–69, May 2013. doi: 10.1109/ICRA.2013.6630557.
- Bickson, D. *Gaussian Belief Propagation: Theory and Application*. PhD thesis, July 2009.
- Davison, A. J. and Ortiz, J. FutureMapping 2: Gaussian Belief Propagation for Spatial AI. *arXiv:1910.14139 [cs]*, October 2019.
- de Vries, B. and Friston, K. J. A Factor Graph Description of Deep Temporal Active Inference. *Frontiers in Computational Neuroscience*, 11, 2017.
- Dellaert, F. and Kaess, M. Factor Graphs for Robot Perception. *Foundations and Trends® in Robotics*, 6(1-2): 1–139, August 2017. doi: 10.1561/23000000043.

- Doucet, A. A Note on Efficient Conditional Simulation of Gaussian Distributions. Technical report, University of British Columbia, 2010.
- Eustice, R. M., Singh, H., and Leonard, J. J. Exactly Sparse Delayed-State Filters for View-Based SLAM. *IEEE Transactions on Robotics*, 22(6):1100–1114, December 2006. doi: 10.1109/TRO.2006.886264.
- Evensen, G. The Ensemble Kalman Filter: Theoretical formulation and practical implementation. *Ocean Dynamics*, 53(4):343–367, November 2003. doi: 10.1007/s10236-003-0036-9.
- Evensen, G. *Data Assimilation - The Ensemble Kalman Filter*. Springer, Berlin; Heidelberg, 2009. ISBN 978-3-642-03711-5 3-642-03711-9. doi: 10.1007/978-3-642-03711-5.
- Ferziger, J. H., Perić, M., and Street, R. L. *Computational Methods for Fluid Dynamics*. Springer, Cham, 4th ed. 2020 edition edition, August 2019. ISBN 978-3-319-99691-2.
- Forney, G. Codes on graphs: Normal realizations. *IEEE Transactions on Information Theory*, 47(2):520–548, February 2001. doi: 10.1109/18.910573.
- Frey, B. J., Kschischang, F. R., Loeliger, H.-A., and Wiberg, N. Factor graphs and algorithms. In *Proceedings of the Annual Allerton Conference on Communication Control and Computing*, volume 35, pp. 666–680. Citeseer, 1997.
- Halko, N., Martinsson, P.-G., and Tropp, J. A. Finding structure with randomness: Probabilistic algorithms for constructing approximate matrix decompositions, December 2010.
- Houtekamer, P. L. and Zhang, F. Review of the Ensemble Kalman Filter for Atmospheric Data Assimilation. *Monthly Weather Review*, 144(12):4489–4532, December 2016. doi: 10.1175/MWR-D-15-0440.1.
- Ihler, A. and McAllester, D. Particle Belief Propagation. In *Proceedings of the Twelfth International Conference on Artificial Intelligence and Statistics*, pp. 256–263. PMLR, April 2009.
- Koller, D. and Friedman, N. *Probabilistic Graphical Models : Principles and Techniques*. MIT Press, Cambridge, MA, 2009. ISBN 0-262-01319-3.
- Kschischang, F. R., Frey, B. J., and Loeliger, H.-A. Factor graphs and the sum-product algorithm. *IEEE Transactions on Information Theory*, 47(2):498–519, February 2001. doi: 10.1109/18.910572.
- Laue, S., Mitterreiter, M., and Giesen, J. Computing Higher Order Derivatives of Matrix and Tensor Expressions. In Bengio, S., Wallach, H., Larochelle, H., Grauman, K., Cesa-Bianchi, N., and Garnett, R. (eds.), *Advances in Neural Information Processing Systems 31*, pp. 2750–2759. Curran Associates, Inc., 2018.
- Laue, S., Mitterreiter, M., and Giesen, J. A simple and efficient tensor calculus. In *AAAI Conference on Artificial Intelligence*, (AAAI). 2020.
- Li, Z., Kovachki, N., Azizzadenesheli, K., Liu, B., Bhattacharya, K., Stuart, A., and Anandkumar, A. Fourier Neural Operator for Parametric Partial Differential Equations. *arXiv:2010.08895 [cs, math]*, October 2020.
- Margossian, C. C. A Review of automatic differentiation and its efficient implementation. *WIREs Data Mining and Knowledge Discovery*, 9(4):e1305, July 2019. doi: 10.1002/WIDM.1305.
- Murphy, K. P., Weiss, Y., and Jordan, M. I. Loopy belief propagation for approximate inference: An empirical study. In *Proceedings of the Fifteenth Conference on Uncertainty in Artificial Intelligence*, UAI’99, pp. 467–475, San Francisco, CA, USA, July 1999. Morgan Kaufmann Publishers Inc. ISBN 978-1-55860-614-2.
- Ortiz, J., Evans, T., and Davison, A. J. A visual introduction to Gaussian Belief Propagation. *arXiv:2107.02308 [cs]*, July 2021.
- Pearl, J. *Probabilistic Reasoning in Intelligent Systems: Networks of Plausible Inference*. The Morgan Kaufmann Series in Representation and Reasoning. Kaufmann, San Francisco, Calif, rev. 2. print., 12. [dr.] edition, 2008. ISBN 978-1-55860-479-7.
- Petersen, K. B. and Pedersen, M. S. *The Matrix Cookbook*. Technical report, 2012.
- Ranganathan, A., Kaess, M., and Dellaert, F. Loopy SAM. In *Proceedings of the 20th International Joint Conference on Artificial Intelligence*, IJCAI’07, pp. 2191–2196, San Francisco, CA, USA, January 2007. Morgan Kaufmann Publishers Inc.
- Sriperumbudur, B. K., Gretton, A., Fukumizu, K., Schölkopf, B., and Lanckriet, G. R. G. Hilbert Space Embeddings and Metrics on Probability Measures. *Journal of Machine Learning Research*, 11:1517–1561, April 2010.
- Vehtari, A., Gelman, A., Sivula, T., Jylänki, P., Tran, D., Sahai, S., Blomstedt, P., Cunningham, J. P., Schiminovich, D., and Robert, C. Expectation propagation as a way of life: A framework for Bayesian inference on partitioned data. *arXiv:1412.4869 [stat]*, November 2019.

- Wainwright, M. J. and Jordan, M. I. *Graphical Models, Exponential Families, and Variational Inference*, volume 1 of *Foundations and Trends® in Machine Learning*. Now Publishers, 2008. doi: 10.1561/2200000001.
- Wand, M. P. Fast Approximate Inference for Arbitrarily Large Semiparametric Regression Models via Message Passing. *Journal of the American Statistical Association*, 112(517):137–168, January 2017. doi: 10.1080/01621459.2016.1197833.
- Weiss, Y. and Freeman, W. T. Correctness of Belief Propagation in Gaussian Graphical Models of Arbitrary Topology. *Neural Computation*, 13(10):2173–2200, October 2001. doi: 10.1162/089976601750541769.
- Wilson, J. T., Borovitskiy, V., Terenin, A., Mostowsky, P., and Deisenroth, M. P. Pathwise Conditioning of Gaussian Processes. *Journal of Machine Learning Research*, 22(105):1–47, 2021.
- Wright, S. The Method of Path Coefficients. *The Annals of Mathematical Statistics*, 5(3):161–215, September 1934. doi: 10.1214/aoms/1177732676.
- Yedidia, J., Freeman, W., and Weiss, Y. Constructing Free-Energy Approximations and Generalized Belief Propagation Algorithms. *IEEE Transactions on Information Theory*, 51(7):2282–2312, July 2005. doi: 10.1109/TIT.2005.850085.
- Yedidia, J. S., Freeman, W. T., and Weiss, Y. Generalized belief propagation. In *Proceedings of the 13th International Conference on Neural Information Processing Systems, NIPS’00*, pp. 668–674, Cambridge, MA, USA, January 2000. MIT Press.
- Zhuo, J., Liu, C., Shi, J., Zhu, J., Chen, N., and Zhang, B. Message Passing Stein Variational Gradient Descent. In *Proceedings of the 35th International Conference on Machine Learning*, pp. 6018–6027. PMLR, July 2018.

A. Benchmark problems

To demonstrate the utility of our method, we select example problems of system identification type, where a latent parameter of interest must be inferred from its effects upon the dynamics of a hidden Markov model. As such it is closely related to, but more challenging than, state filtering.

Throughout, unless otherwise specified, the hyper parameters of the algorithms are $\gamma^2 = 0.01$ and $\sigma^2 = 0.001$ for both GaBP and GEnBP. GEnBP has additional hyperparameters $\eta^2 = 0.1$ and $N = 64$. We cap the number of iterations of message-propagation descent steps at 150. We relinearise or re-simulate after 10 message-propagation steps.

A.1. System identification

In the system identification problem our goal is to estimate the time-invariant latent system parameter \mathbf{q} . This parameter influences all states in the Hidden Markov Model, where \mathbf{x}_0 represents the unobserved initial state, and subsequent states $\mathbf{x}_1, \mathbf{x}_2, \dots$ evolve over time. Each state \mathbf{x}_i is associated with an observed state \mathbf{y}_i , as depicted in Figure 4.

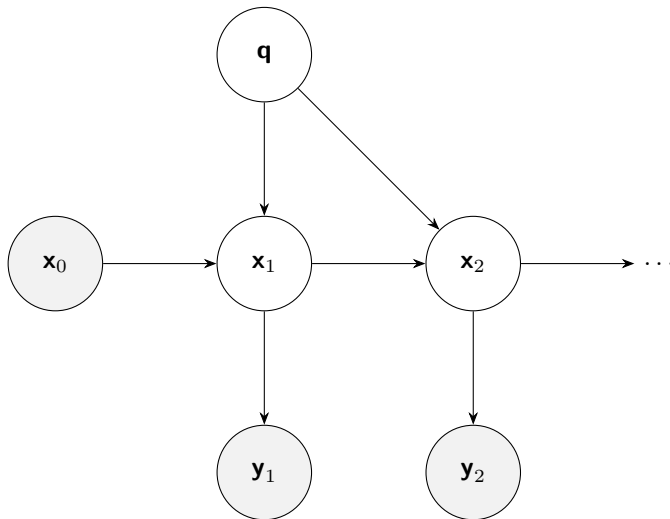


Figure 4: Generative model for the system identification problem, with latent system parameter \mathbf{q} , where all states depend on \mathbf{q} and the previous state. Observed states are shaded.

A.2. 1D transport problem

States are one-dimensional vectors of length $D_{\mathcal{Q}}$.

$$\begin{aligned} \mathcal{P}_{\mathbf{x}}(\mathbf{x}_{t-1}, \mathbf{q}) &:= \text{shift}_k(g\mathbf{x}_{t-1} + (1-g)\mathbf{q} * \mathbf{b}) + \epsilon_{\text{process}} \\ \mathcal{P}_{\mathbf{y}}(\mathbf{x}_t) &:= \text{downsample}_{\ell}(\mathbf{x}_t) + \epsilon_{\text{obs}} \end{aligned}$$

$\mathcal{P}_{\mathbf{q}}$, the prior for \mathbf{q} , draws periodic functions of the form $F(\theta; \mu, \kappa, A) = A \cdot e^{\kappa \cos(\frac{k * 2\pi}{D_{\mathcal{Q}}} - \mu)}$ for $k \in \{0, 1, D_{\mathcal{Q}} - 1\}$, where $\mu \sim \text{Uniform}[0, 2\pi]$, is the phase, $\kappa \sim \chi^2(\sqrt{2\pi})$, and $A = 9$, i.e. the prior belief about amplitude is diffuse, but encodes smoothness and periodicity. downsample_{ℓ} is a downsampling operator, which takes every ℓ th element of the input vector.

The inference problem is to estimate the parameter \mathbf{q} given the sequence of observations $\{\mathbf{y}_t\}$ and the initial state \mathbf{x}_0 .

The number of timesteps is $T = 10$.

A.3. Navier-Stokes system

The Navier-Stokes equation defines a classic problem in fluid modeling, whose solution is of interest in many engineering applications. A full introduction to the Navier-Stokes equation is beyond the scope of this paper; see Ferziger et al. (2019) or one of the many other introductions.

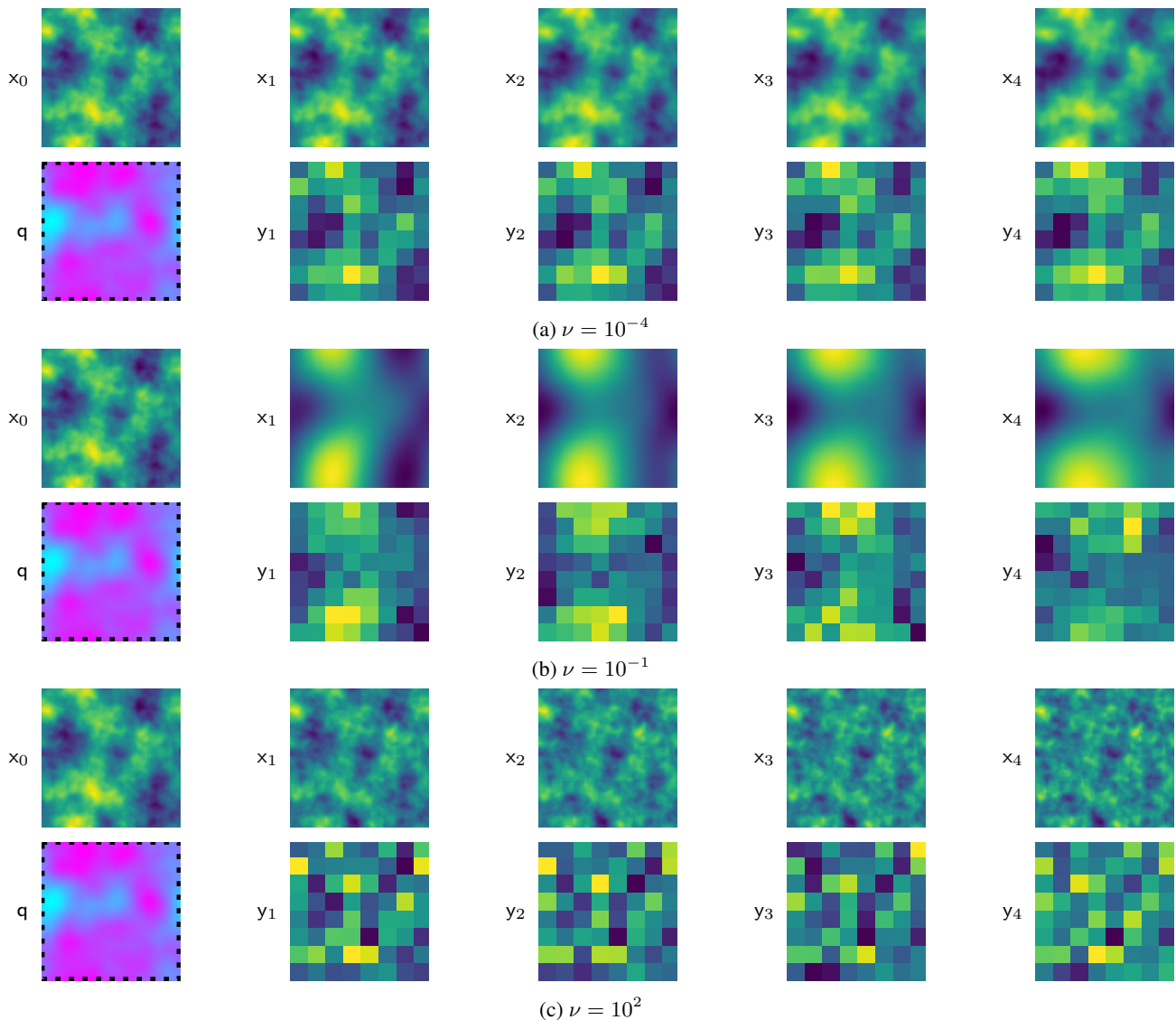


Figure 5: Three different Navier-Stokes simulations, with $\Delta t = 0.2$ and varying value of viscosity ν . The simulation is run on a 64×64 grid; observations are 8×8 and corrupted by white Gaussian noise with st $\sigma = 0.1$ relative to a normalize unit scale for the simulations.

Our implementation here is a 2D incompressible flow, solved using a spectral method with pytorch implementation from a simulator Li et al. (2020). Defining vorticity $\omega = \frac{\partial v}{\partial x} - \frac{\partial u}{\partial y}$ and streamfunction ψ which generates the velocity field by

$$u = \frac{\partial \psi}{\partial y}$$

$$v = -\frac{\partial \psi}{\partial x}$$

the Navier Stokes equations are

1. Poisson equation $\nabla^2 \psi = -\omega$
2. Vorticity equation $\frac{\partial \omega}{\partial t} + u \frac{\partial \omega}{\partial x} + v \frac{\partial \omega}{\partial y} = \nu \nabla^2 \omega$

The discretisation of the equation is onto an $d \times d$ finite element basis for the domain, where each point summarises the vorticity field at that point. At each discretised time-step we inject additive mean-zero (d^2)-dimensional Gaussian white noise $\boldsymbol{\nu}_t \sim \mathcal{N}(\mathbf{0}, \sigma_\eta^2 \mathbf{I})$ and static forcing term \mathbf{q} to the velocity term before solving the equation.

2d matrices are represented as 2d vectors by stacking and unstacking as needed, so $\mathbf{x}_t = \text{vec}(\psi)$. $\mathbf{y} = \text{downsample}_\ell(\mathbf{x}_t) + \boldsymbol{\eta}$, where $\boldsymbol{\eta} \sim \mathcal{N}(\mathbf{0}, \sigma_\eta^2 \mathbf{I})$ is the observation noise.

Initial state and forcings are sampled from a discrete periodic Gaussian random field with

$$PSD(k) = \sigma^2 (4\pi^2 \|k\|^2 + \tau^2)^{-\alpha}. \tag{30}$$

B. Experimental details and additional results

B.1. Hardware configuration

Timings are conducted on Dell PowerEdge C6525 Server AMD EPYC 7543 32-Core Processors running at 2.8 GHz (3.7 GHz turbo) with 256 MB cache. Float precision is set to 64 bits for all calculations. Memory limit is capped to 32Gb. Execution time is capped to 119 minutes.

B.2. Ensemble size

In the main text, we have left the matter of ensemble size N open. On one hand, ensembles of order $N \approx 10^2$ seem to be ample for the problems we have considered. We might be concerned that the trade-off of increasing ensemble size is unclear; on one hand many computational costs scale relatively simply as $\mathcal{O}(D^N 2 + N^3)$ (App I). On the other, we do not know how much extra precision we gain in general by increasing N . In Fig. 6 we show a small experiment to examine this trade-off, where the ensemble size is increased from $N = 16$ to $N = 512$ in steps of size 16. The problem shows a rapid improvement as the ensemble increases to $N = 64$, but diminishing marginal returns. There is no clear cut-off as such, but we specify $N = 64$ as a default value for the experiments in the main text.

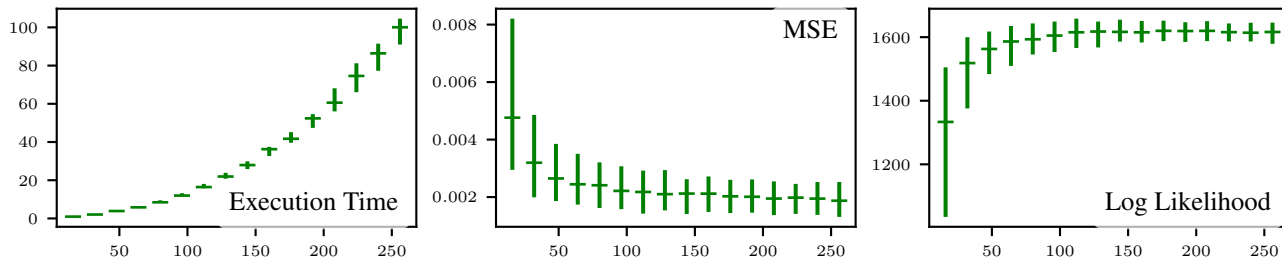


Figure 6: Performance of GENBP with varying ensemble size N for the 1d transport system identification problem (App A.2). Confidence intervals are empirical 95% intervals based on $n = 80$ independent runs.

C. Minimum viable introduction to probabilistic graphical models

The field of probabilistic graphical models is mature and vast. We refer the reader to Koller & Friedman (e.g. 2009); Wainwright & Jordan (e.g. 2008, and references therein) for a thorough introduction. A miniature introduction sufficient for this paper may be found here.

For the purposes of the current paper, it is sufficient to understand that this is the framework that we use to enable inference in complicated hierarchical systems with partial observations. Consider, for example, the hierarchical process in Fig. 7, which is a simplified representation of a weather model. An oceanic physics simulator and an atmospheric physics simulator provide forward predictions of the state of the ocean and atmosphere, and influence each other through physical coupling. Each of these dynamic systems is observed on a different time schedule by some form of telemetry (thermal satellite imagery for the oceans, phase radar for the atmosphere). All observations and state are high-dimensional, noisy and governed by nonlinear partial differential equations, including the observation models. Our primary target of inference is the 1-step ahead forward prediction for the atmosphere model. We could imagine many extensions of this, for example, to simultaneously learn the parameters of the observation or physics models as we learn their states.

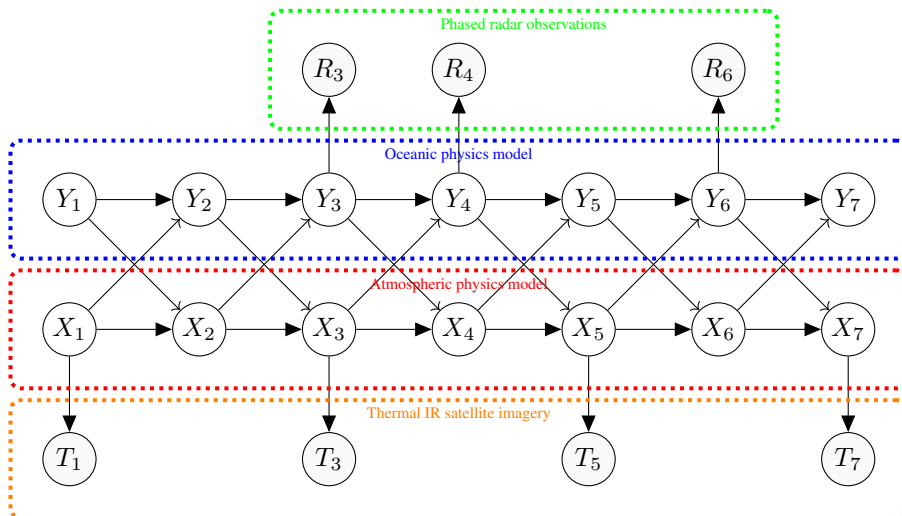


Figure 7: A complicated graphical model structure arising from a weather prediction problem. The model includes an oceanic physics simulator, an atmospheric physics simulator, phased radar observations, and thermal IR satellite imagery. The model is high-dimensional, noisy, and governed by nonlinear partial differential equations.

Graphical model formalisms provide a means of estimating states and parameters in these systems; the essential idea is that if we can find a set of rules that work for inference for arbitrary models, then we can apply them to complicated models like this. This paper introduces such a generic set of rules, which in-principle applies to arbitrarily complex graphical models, although scaling up to the complexity of the model in Fig. 7 is out of scope for a short methodological paper such as this.

C.1. Directed graphs and factor graphs

We begin with the structural equations defining the model. By sampling from the distribution over these ancestral variables then iteratively applying the generative model (31), we obtain samples from the joint prior distribution of all random variates from the model. The state is jointly

$$\mathbf{x} = \begin{bmatrix} \mathbf{x}_{\mathcal{O}_1} \\ \vdots \\ \mathbf{x}_{\mathcal{O}_J} \end{bmatrix} = \begin{bmatrix} \mathcal{P}_1(\mathbf{x}_{\mathcal{I}_1}) \\ \vdots \\ \mathcal{P}_J(\mathbf{x}_{\mathcal{I}_J}) \end{bmatrix}. \quad (31)$$

The following conditions must hold for this to define a valid structural equation model

1. $\forall j, \mathcal{O}_j \cap \mathcal{I}_j = \emptyset$ (no self-loop in a step).
2. If $v \in \mathcal{O}_j$, then for $k > j$, v appears only in \mathcal{I}_k .

This defines a directed acyclic graph (DAG) over the variables, where the nodes are the variables and the edges are the generating equations. Each generating equation j induces an associated density $p(\mathbf{x}_{\mathcal{O}_j} | \mathbf{x}_{\mathcal{I}_j})$. The associated joint density is

$$p(\mathbf{x}) = \prod_j p(\mathbf{x}_{\mathcal{O}_j} | \mathbf{x}_{\mathcal{I}_j}). \quad (32)$$

Under some mild technical conditions (the local Markov condition, faithfulness and consistence - see Koller & Friedman (2009)), the representation given by the graph and the structural equations is equivalent to the joint distribution over the variables; We assume these conditions throughout.

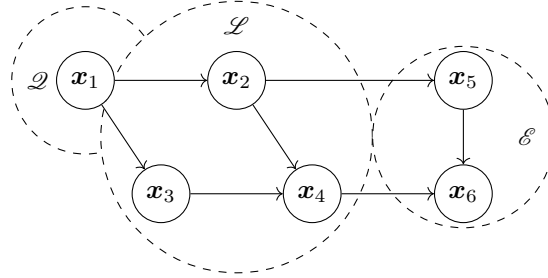
Hereafter we use the following specific generative model as a running example:

$$\begin{bmatrix} \mathbf{x}_1 \\ \mathbf{x}_2 \\ \mathbf{x}_3 \\ \mathbf{x}_4 \\ \mathbf{x}_5 \\ \mathbf{x}_6 \end{bmatrix} = \begin{bmatrix} \mathcal{P}_1() \\ \mathcal{P}_{12}(\mathbf{x}_1) \\ \mathcal{P}_{12}(\mathbf{x}_1) \\ \mathcal{P}_{234}(\mathbf{x}_2, \mathbf{x}_3) \\ \mathcal{P}_{25}(\mathbf{x}_2) \\ \mathcal{P}_{456}(\mathbf{x}_4, \mathbf{x}_5) \end{bmatrix}. \quad (33)$$

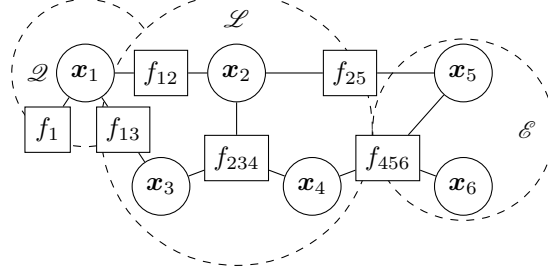
It is diagrammed in Fig 8 as a running example of the formalism. Its associated density can be factorised as

$$p(\mathbf{x}) = p_1(\mathbf{x}_1)p_{12}(\mathbf{x}_2|\mathbf{x}_1)p_{13}(\mathbf{x}_3|\mathbf{x}_1)p_{25}(\mathbf{x}_5|\mathbf{x}_2)p_{234}(\mathbf{x}_4|\mathbf{x}_2, \mathbf{x}_3)p_{456}(\mathbf{x}_6|\mathbf{x}_4, \mathbf{x}_5). \quad (34)$$

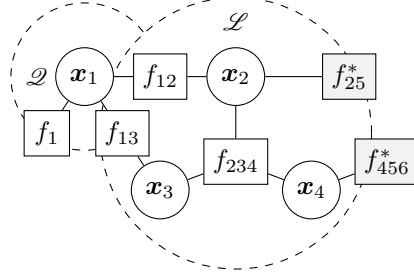
The directed generative model \mathcal{M} , and equivalently, conditional density, corresponds to 8a.



(a) Prior directed graph of generative model \mathcal{M} , $p(\mathbf{x}) = p_1(\mathbf{x}_1)p_{12}(\mathbf{x}_2|\mathbf{x}_1)p_{13}(\mathbf{x}_3|\mathbf{x}_1)p_{25}(\mathbf{x}_5|\mathbf{x}_2)p_{234}(\mathbf{x}_4|\mathbf{x}_2, \mathbf{x}_3)p_{456}(\mathbf{x}_6|\mathbf{x}_4, \mathbf{x}_5)$.



(b) Prior factor graph \mathcal{G} for generative model \mathcal{M} , $p(\mathbf{x}) = f_1(\mathbf{x}_1)f_{12}(\mathbf{x}_1, \mathbf{x}_2)f_{13}(\mathbf{x}_1, \mathbf{x}_3)f_{234}(\mathbf{x}_2, \mathbf{x}_3, \mathbf{x}_4)f_{25}(\mathbf{x}_2, \mathbf{x}_5)f_{456}(\mathbf{x}_4, \mathbf{x}_5, \mathbf{x}_6)$.



(c) Posterior factor graph \mathcal{G}^* of generative model \mathcal{M} after observing \mathbf{x}_5 and \mathbf{x}_6 , $p(\mathbf{x}_1, \mathbf{x}_2, \mathbf{x}_3, \mathbf{x}_4|\mathbf{x}_5, \mathbf{x}_6) \propto f_1(\mathbf{x}_1)f_{12}(\mathbf{x}_1, \mathbf{x}_2)f_{13}(\mathbf{x}_1, \mathbf{x}_3)f_{234}(\mathbf{x}_2, \mathbf{x}_3, \mathbf{x}_4)f_{25}^*(\mathbf{x}_2)f_{456}^*(\mathbf{x}_4)$

Figure 8: The graphical model variants used in this paper for example model (8): (a) prior generative graph, (b) prior factor graph, and (c) posterior factor graph; each with query nodes $\mathcal{Q} = \{1\}$, latent nodes $\mathcal{L} = \{2, 3, 4\}$, and observed nodes $\mathcal{E} = \{5, 6\}$.

The directed graphical model has the advantage of being intuitive, but it is not the most convenient for inference.

The factor graph form (Frey et al., 1997; Kschischang et al., 2001) discards the directions of the arrows induced by the generative models and works only with generic factors, transforming

$$p(\mathbf{x}_1|\mathbf{x}_2) \rightarrow f(\mathbf{x}_1, \mathbf{x}_2). \quad (35)$$

Our running example (34) becomes

$$p(\mathbf{x}) = f_1(\mathbf{x}_1)f_{12}(\mathbf{x}_1, \mathbf{x}_2)f_{13}(\mathbf{x}_1, \mathbf{x}_3)f_{234}(\mathbf{x}_2, \mathbf{x}_3, \mathbf{x}_4)f_{25}(\mathbf{x}_2, \mathbf{x}_5)f_{456}(\mathbf{x}_4, \mathbf{x}_5, \mathbf{x}_6). \quad (36)$$

The corresponding factor graph is shown in Fig. 8b. The factor graph is a bipartite graph with nodes corresponding to both variables and factor nodes. This representation has the advantage that simple approximate belief-updating message-passing rules may be written down for it. These rules we introduce in a sec. C.2.

We introduce one final graph transformation of use in this paper, which produces the conditional graph. We recall (3) that in practice we are interested in the evidence-conditional, posterior distribution, $\mathbf{x}_{\mathcal{Q}}$ given the evidence variables $\mathbf{x}_{\mathcal{E}} = \mathbf{x}_{\mathcal{E}}^*$, i.e.

$$p(\mathbf{x}_{\mathcal{Q}}|\mathbf{x}_{\mathcal{E}}=\mathbf{x}_{\mathcal{E}}^*) = \frac{p(\mathbf{x}_{\mathcal{Q}}, \mathbf{x}_{\mathcal{E}}=\mathbf{x}_{\mathcal{E}}^*)}{p(\mathbf{x}_{\mathcal{E}}=\mathbf{x}_{\mathcal{E}}^*)} \quad (37)$$

$$= \frac{\int p(\mathbf{x}_{\mathcal{Q}}, \mathbf{x}_{\mathcal{L}}, \mathbf{x}_{\mathcal{E}}=\mathbf{x}_{\mathcal{E}}^*)d\mathbf{x}_{\mathcal{L}}}{\int p(\mathbf{x}_{\mathcal{Q}}, \mathbf{x}_{\mathcal{L}}, \mathbf{x}_{\mathcal{E}}=\mathbf{x}_{\mathcal{E}}^*)d\mathbf{x}_{\mathcal{Q}}d\mathbf{x}_{\mathcal{L}}}. \quad (38)$$

This can also be represented as a factor graph, as shown in Fig. 8c. The rule in this case is simply to use the factor graph corresponding to the factorisation induced by the posterior, which has a slightly different set of factors, since the observed nodes are no longer random, e.g.

$$p(\mathbf{x}_{\mathcal{Q}}|\mathbf{x}_{\mathcal{E}}=\mathbf{x}_{\mathcal{E}}^*) \propto p_1(\mathbf{x}_1)p_{12}(\mathbf{x}_2|\mathbf{x}_1)p_{13}(\mathbf{x}_3|\mathbf{x}_1)p_{234}(\mathbf{x}_4|\mathbf{x}_2, \mathbf{x}_3)p_{25}(\mathbf{x}_2|\mathbf{x}_5=\mathbf{x}_5^*)p_{456}(\mathbf{x}_4|\mathbf{x}_5=\mathbf{x}_5^*, \mathbf{x}_6=\mathbf{x}_6^*) \quad (39)$$

$$\propto f_1(\mathbf{x}_1)f_{12}(\mathbf{x}_1, \mathbf{x}_2)f_{13}(\mathbf{x}_1, \mathbf{x}_3)f_{234}(\mathbf{x}_2, \mathbf{x}_3, \mathbf{x}_4)f_{25}^*(\mathbf{x}_2)f_{456}^*(\mathbf{x}_4). \quad (40)$$

C.2. Factor Graph Gaussian Belief Propagation

Basic loopy belief propagation (Murphy et al., 1999) is a simple and efficient algorithm for approximate inference of marginals over certain variables in factor graphs. There is a rich literature on when and how this algorithm converges to the true marginal, (Wainwright & Jordan, 2008; Yedidia et al., 2005). We do not concern ourselves with those details in this work, but simply follow industrial practice (e.g. Dellaert & Kaess, 2017) in treating it as a good enough approximation for our purposes. Following the terminology of Ortiz et al. (2021).

Proposition 1 (Belief Propagation on Factor Graphs). *The following messages,*

$$m_{f_j \rightarrow \mathbf{x}_k} = \int \left(f_j(\mathbf{x}_{\mathcal{N}_j}) \prod_{i \in \mathcal{N}_j \setminus k} m_{\mathbf{x}_i \rightarrow f_j} \right) d\mathbf{x}_{\mathcal{N}_j \setminus k} \quad (5)$$

$$m_{\mathbf{x}_k \rightarrow f_j} = \prod_{s \in \mathcal{N}_k \setminus j} m_{f_s \rightarrow \mathbf{x}_k}, \quad (6)$$

iteratively and synchronously propagated between all the nodes in the associated factor graph, yield the approximate marginal at target variable node,

$$b_{\mathcal{G}}(\mathbf{x}_k) = \prod_{s \in \mathcal{N}_k} m_{f_s \rightarrow \mathbf{x}_k} = \int p(\mathbf{x})d\mathbf{x}_{\setminus k}. \quad (7)$$

The fixed points of this iteration are the fixed points of the Bethe approximation to the target marginal.

The factor graph belief propagation algorithm for generic factor graphs using these messages is presented Algorithm 3.

C.3. Gaussian Factor updates

Finally we note that the factor graph formalism is particularly convenient for Gaussian models, as the Gaussian density is closed under multiplication, conditioning and marginalisation. We introduced this in sec 2.2.3, but write it out in full here.

As an exponential family distribution (Wainwright & Jordan, 2008), it become convenient to work with Gaussians in canonical form Eustice et al. (2006). We write $\phi_M(\mathbf{x}; \mathbf{m}, \mathbf{K})$ for ϕ_M the Gaussian density with moment parameters mean \mathbf{m} and covariance \mathbf{K} .

Algorithm 3 Loopy Low-rank Belief Propagation over Factor Graph \mathcal{G}

Require: Factor graph \mathcal{G} with variable nodes $\{\mathbf{x}_k\}_k$ and factor nodes $\{f_j\}_j$
Require: Initial messages $\mathbf{x}_k \rightarrow f_j$ and $f_j \rightarrow \mathbf{x}_k$
Ensure: Approximate marginal beliefs $b(\mathbf{x}_k)$ for all $\mathbf{x}_k \in \mathcal{G}$

- 1: Initialize message queues $Q_{\mathbf{x}_k \rightarrow f_j}$ and $Q_{f_j \rightarrow \mathbf{x}_k}$ to be empty
- 2: **while** not converged **do**
- 3: **for** each factor $f_j \in \mathcal{G}$ **do**
- 4: **for** each variable $\mathbf{x}_k \in \mathcal{N}_{f_j}$ **do**
- 5: Send factor to variable message (5) to each neighbour
- 6: **end for**
- 7: **end for**
- 8: **for** each variable $\mathbf{x}_k \in \mathcal{G}$ **do**
- 9: **for** each factor $f_j \in \mathcal{N}_{\mathbf{x}_k}$ **do**
- 10: Send variable to factor message (6) to each neighbour
- 11: **end for**
- 12: Update belief $b(\mathbf{x}_k)$ (7)
- 13: **end for**
- 14: Check for convergence criteria
- 15: **end while**
- 16: Return $b(\mathbf{x}_k)$ for all $\mathbf{x}_k \in \mathcal{G}$

Proposition 6. As in Proposition 1, we partition the random vector $\mathbf{x}_j \sim \phi_M \left(\begin{bmatrix} \mathbf{x}_k \\ \mathbf{x}_\ell \end{bmatrix}; \begin{bmatrix} \mathbf{m}_k \\ \mathbf{m}_\ell \end{bmatrix}, \begin{bmatrix} \mathbf{K}_{kk} & \mathbf{K}_{k\ell} \\ \mathbf{K}_{\ell k} & \mathbf{K}_{\ell\ell} \end{bmatrix} \right)$. We define $\hat{\mathbf{K}} := (\mathbf{K}_{jj}^{-1} + \mathbf{K}'_{jj}{}^{-1})^{-1}$. Where the node and factors are Gaussian, the operations of Proposition 1 have the following form,

$$\text{Conditioning: } \phi_M(\mathbf{x}_j; \mathbf{m}_j, \mathbf{K}_{jj}), \mathbf{x}_k^* \mapsto \phi_M(\mathbf{x}_\ell; \mathbf{m}_\ell + \mathbf{K}_{\ell k} \mathbf{K}_{kk}^{-1}(\mathbf{x}_k^* - \mathbf{m}_k), \mathbf{K}_{\ell\ell} - \mathbf{K}_{\ell k} \mathbf{K}_{kk}^{-1} \mathbf{K}_{k\ell}); \quad (41)$$

$$\text{Marginalisation: } \phi_M(\mathbf{x}_j; \mathbf{m}_j, \mathbf{K}_{jj}) \mapsto \phi_M(\mathbf{x}_k; \mathbf{m}_k, \mathbf{K}_{kk}); \quad (42)$$

$$\text{Multiplication: } \phi'_M(\mathbf{x}_j; \mathbf{m}'_j, \mathbf{K}'_{jj}), \phi_M(\mathbf{x}_k; \mathbf{m}_k, \mathbf{K}_{kk}) \mapsto \phi_M(\mathbf{x}_j; \hat{\mathbf{K}}(\mathbf{K}_{jj}^{-1} \mathbf{m}_j + \mathbf{K}'_{kk}{}^{-1} \mathbf{m}'_j), \hat{\mathbf{K}}); \quad (43)$$

$$\phi'_C(\mathbf{x}_j; \mathbf{n}'_j, \mathbf{P}'_{jj}), \phi_C(\mathbf{x}_k; \mathbf{n}_k, \mathbf{P}_{kk}) \mapsto \phi_C(\mathbf{x}_j; \mathbf{n}'_j + \mathbf{n}_j, \mathbf{P}' + \mathbf{P}). \quad (44)$$

Proof. e.g. Bickson (2009). □

The classic GaBP algorithm is in fact more complicated than this just the application of these rules, in practice incorporating additional hyperparameters and rules for convergence. Most importantly, since GaBP is frequently applied to factors that are not truly Gaussian, it needs a rule for finding a Gaussian distribution which approximates some factor potential. This is classically Taylor-expansion-type linearisation about the mean, a.k.a. propagation of errors and is introduced in the main body of the text at (15). Taylor expansion is not the only choice, a fact which GEnBP exploits heavily.

D. Minimum viable introduction to the Ensemble Kalman Filter

The field of Ensemble Kalman methods is mature and vast. We refer the reader to e.g. Evensen (2009) and references therein for a thorough introduction. A miniature introduction sufficient for this paper may be found here.

The central idea is the following: given the state-space model (Fig. 9) with hidden states \mathbf{x}_t and observations \mathbf{y}_t , we wish to estimate the hidden states given the observations. The joint prior density of the state and observations is

$$p(\mathbf{x}_1, \mathbf{x}_2, \dots, \mathbf{x}_T, \mathbf{y}_1, \mathbf{y}_2, \dots, \mathbf{y}_T) =: p(\mathbf{x}_{0:T}, \mathbf{y}_{1:T}) \quad (45)$$

$$= \prod_{t=1}^T p(\mathbf{x}_t | \mathbf{x}_{t-1}) p(\mathbf{y}_t | \mathbf{x}_t). \quad (46)$$

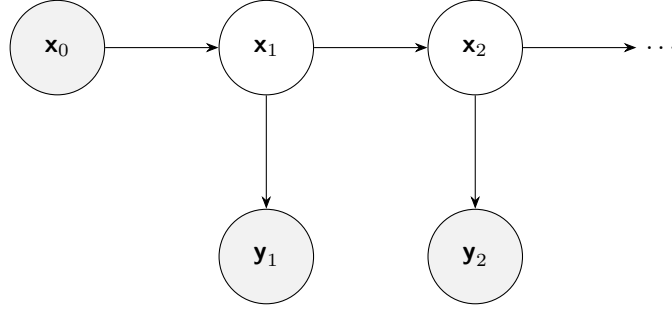


Figure 9: Generative model for state filtering problem, hidden states \mathbf{x}_t and observation \mathbf{y}_t for $t = 1, 2, \dots$

Filtering leverages the fact that

$$p(\mathbf{x}_{0:T}, \mathbf{y}_{1:T}) = p(\mathbf{y}_T | \mathbf{x}_T) p(\mathbf{x}_T | \mathbf{x}_{T-1}) p(\mathbf{x}_{1:T-1}, \mathbf{y}_{1:T}) \quad (47)$$

so we can solve the problem by induction,

$$p(\mathbf{x}_{0:T} | \mathbf{y}_{1:T}) \propto p(\mathbf{y}_T | \mathbf{x}_T) p(\mathbf{x}_T | \mathbf{x}_{T-1}) p(\mathbf{x}_{1:T-1}, \mathbf{y}_{1:T-1}) \quad (48)$$

$$\propto p(\mathbf{y}_T | \mathbf{x}_T) p(\mathbf{x}_T | \mathbf{x}_{T-1}) p(\mathbf{x}_{T-1} | \mathbf{y}_{1:T-1}). \quad (49)$$

If we know $p(\mathbf{x}_{1:T-1} | \mathbf{y}_{1:T-1})$, to update to a new estimate of $p(\mathbf{x}_T | \mathbf{y}_{1:T})$ we only need to be able to multiply its density by $p(\mathbf{x}_T | \mathbf{x}_{T-1}) p(\mathbf{y}_T | \mathbf{x}_T)$ and normalize; thus we can always calculate an estimate of the new state given the previous state estimate and the current observations.

Under Gaussianity of all distributions and linearity of all processes (e.g. Petersen & Pedersen (2012)) we can represent this density update in terms of the distribution parameters. For some $\mathbf{m}_{T-1}, \mathbf{K}_{T-1}$,

$$p(\mathbf{x}_{T-1} | \mathbf{y}_{1:T-1}) = \phi_M(\mathbf{x}_{T-1}; \mathbf{m}_{T-1}, \mathbf{K}_{T-1}) \quad (50)$$

Linearity implies that there exist $\mathbf{d}_{T-1}, \mathbf{F}_{T-1}, \mathbf{Q}_T$ the forward propagation operator $\mathbf{x}_T = \mathcal{P}_{T-1}(\mathbf{x}_{T-1})$ of \mathbf{x}_T is

$$\mathbf{x}_T | \mathbf{x}_{T-1} = \mathcal{P}(\mathbf{x}_{T-1}) \quad (51)$$

$$= \mathbf{F}_{T-1} \mathbf{x}_{T-1} + \mathbf{d}_{T-1} + \boldsymbol{\epsilon}_T \quad (52)$$

where $\boldsymbol{\epsilon} \sim \mathcal{N}(\mathbf{0}, \mathbf{Q}_T)$ so that

$$p\left(\begin{bmatrix} \mathbf{x}_{T-1} \\ \mathbf{x}_T \end{bmatrix} \middle| \mathbf{y}_{1:T-1}\right) = \phi_M\left(\begin{bmatrix} \mathbf{x}_{T-1} \\ \mathbf{x}_T \end{bmatrix}; \begin{bmatrix} \mathbf{m}_{T-1} \\ \mathbf{d}_{T-1} + \mathbf{F}_{T-1} \mathbf{m}_{T-1} \end{bmatrix}, \begin{bmatrix} \mathbf{K}_{T-1} & \mathbf{K}_{T-1} \mathbf{F}_{T-1}^\top \\ \mathbf{F}_{T-1} \mathbf{K}_{T-1} & \mathbf{F}_{T-1} \mathbf{K}_{T-1} \mathbf{F}_{T-1}^\top + \mathbf{Q}_T \end{bmatrix}\right). \quad (53)$$

The \mathbf{x}_T marginal is again Gaussian,

$$p(\mathbf{x}_T | \mathbf{x}_{T-1}, \mathbf{y}_{1:T-1}) = \phi_M(\mathbf{x}_T; \tilde{\mathbf{m}}_T, \tilde{\mathbf{K}}_T) \quad (54)$$

for $\tilde{\mathbf{m}}_T = \mathbf{F}_{T-1} \mathbf{m}_{T-1} + \mathbf{d}_{T-1}$ and $\tilde{\mathbf{K}}_T = \mathbf{F}_{T-1} \mathbf{K}_{T-1} \mathbf{F}_{T-1}^\top + \mathbf{Q}_T$.

It remains to condition on the observation \mathbf{y}_T . We suppose that the measurement model $\mathbf{y}_T = \mathcal{H}_T(\mathbf{x}_T)$ is linear and Gaussian, so that

$$\mathbf{y}_T | \mathbf{x}_T = \mathcal{H}(\mathbf{x}_T) \quad (55)$$

$$= \mathbf{H}_T \mathbf{x}_T + \mathbf{e}_T + \boldsymbol{\varepsilon}_T \quad (56)$$

where $\boldsymbol{\varepsilon}_T \sim \mathcal{N}(\mathbf{0}, \mathbf{R}_T)$. The joint density of \mathbf{x}_T and \mathbf{y}_T is

$$p\left(\begin{bmatrix} \mathbf{x}_T \\ \mathbf{y}_T \end{bmatrix} \middle| \mathbf{y}_{1:T-1}\right) = \phi_M\left(\begin{bmatrix} \mathbf{x}_T \\ \mathbf{y}_T \end{bmatrix}; \begin{bmatrix} \tilde{\mathbf{m}}_T \\ \mathbf{H}_T \tilde{\mathbf{m}}_T + \mathbf{e}_T \end{bmatrix}, \begin{bmatrix} \tilde{\mathbf{K}}_T & \tilde{\mathbf{K}}_T \mathbf{H}_T^\top \\ \mathbf{H}_T \tilde{\mathbf{K}}_T & \mathbf{H}_T \tilde{\mathbf{K}}_T \mathbf{H}_T^\top + \mathbf{R}_T \end{bmatrix}\right). \quad (57)$$

but we can use the standard formula for conditional Gaussian distributions to write

$$p(\mathbf{x}_T | \mathbf{y}_{1:T}) = \phi_M(\mathbf{x}_T; \mathbf{m}_T, \mathbf{K}_T) \quad (58)$$

where

$$\mathbf{K}_T = \tilde{\mathbf{K}}_T - \tilde{\mathbf{K}}_T \mathbf{H}_T (\mathbf{H}_T \tilde{\mathbf{K}}_T \mathbf{H}_T^\top + \mathbf{R}_T)^{-1} \mathbf{H}_T^\top \tilde{\mathbf{K}}_T^\top \quad (59)$$

$$\mathbf{m}_T = \tilde{\mathbf{m}}_T + \mathbf{K}_T \mathbf{H}_T^\top (\mathbf{H}_T \tilde{\mathbf{K}}_T \mathbf{H}_T^\top + \mathbf{R}_T)^{-1} (\mathbf{y}_T - \mathbf{H}_T \tilde{\mathbf{m}}_T - \mathbf{e}_T). \quad (60)$$

i.e. there is a closed-form update.

In practice, we may want to apply this method where at least one of the the state transition and observation models is nonlinear. The Extended Kalman Filter (EKF), uses a linearization of the state transition and observation models to approximate the update. We instead find a linear approximation to the state transition (52) and observation (56) models, by propagation of errors, setting

$$\mathbf{d}_{T-1} \approx \mathbb{E}[\mathcal{P}_{T-1}(\mathbf{m}_{T-1})] \quad (61)$$

$$\mathbf{F}_{T-1} \approx \nabla_{\mathbf{x}_{T-1}} \mathbb{E}[\mathcal{P}_{T-1}(\mathbf{m}_{T-1})] \quad (62)$$

$$\mathbf{e}_T \approx \mathbb{E}[\mathcal{H}_T(\tilde{\mathbf{m}}_T)] \quad (63)$$

$$\mathbf{H}_T \approx \nabla_{\mathbf{x}_T} \mathbb{E}[\mathcal{H}_T(\tilde{\mathbf{m}}_T)]. \quad (64)$$

and $\mathbf{Q}_T = \sigma^2 \mathbf{I}$, $\mathbf{R}_T = \gamma^2 \mathbf{I}$ are set to some diagonal covariance matrices. This type of linearised approximation is also used in the GaBP algorithm.

The EnKF takes a different approach to approximate inference, finding sample-based alternatives to the forward-propagation (54) and the observations update (58) Where the GaBP and EKF method summarises inference in terms of the parameters of a Gaussian distribution, the EnKF summarises the joint distribution in terms of an *ensemble* of Monte Carlo samples, i.e. a matrix of N samples, $\mathbf{X} := [\mathbf{x}^{(n)}]_{1 \leq n \leq N}$ drawn i.i.d. from the prior distribution, $\mathbf{x}^{(n)} \sim \phi_M(\mathbf{x}; \mathbf{m}, \mathbf{K})$. We reprise the definitions introduced in 2.3 by which the statistics of ensemble \mathbf{X} define an implied Gaussian density, $\mathbf{x} \sim \phi_M(\mathbf{x}; \bar{\mathbf{X}}, \widehat{\text{Var}}_V \mathbf{X})$.

$$\mathbf{A}_N := \left[\frac{1}{N} \quad \cdots \quad \frac{1}{N} \right]^\top,$$

$$\mathbf{B}_N := [1 \quad \cdots \quad 1]$$

$$\mathbf{C}_N := \mathbf{I}_N - \mathbf{A}_N \mathbf{B}_N$$

$$\bar{\mathbf{X}} := \mathbf{X} \mathbf{A}_N$$

$$\text{Ensemble mean} \quad (17)$$

$$\check{\mathbf{X}} := \mathbf{X} - \mathbf{X} \mathbf{A}_N \mathbf{B}_N = \mathbf{X} \mathbf{C}_N.$$

$$\text{Ensemble deviation} \quad (18)$$

$$\widehat{\mathbb{E}} \mathbf{X} = \bar{\mathbf{X}} \quad (19)$$

$$\widehat{\text{Var}}_V \mathbf{X} = \frac{1}{N-1} \check{\mathbf{X}} \check{\mathbf{X}}^\top + \mathbf{V} \quad (20)$$

$$\widehat{\text{Cov}}(\mathbf{X}, \mathbf{Y}) = \frac{1}{N-1} \check{\mathbf{X}} \check{\mathbf{Y}}^\top \quad (21)$$

\mathbf{V} is a diagonal matrix *nugget* term, typically set to $\sigma^2 \mathbf{I}$.

The EnKF equivalent of the Kalman filter forward joint distribution (53) is then

$$\begin{bmatrix} \mathbf{X}_{T-1} \\ \mathbf{X}_T \end{bmatrix} \Big| \mathbf{y}_{1:T-1} = \begin{bmatrix} \mathbf{X}_{T-1} | \mathbf{y}_{1:T-1} \\ \mathcal{P}(\mathbf{X}_T | \mathbf{y}_{1:T-1}) \end{bmatrix}. \quad (65)$$

By assumption this means that if we wished to calculate the density of the joint state, it would be

$$p(\mathbf{x}_{T-1}, \mathbf{x}_T | \mathbf{y}_{1:T-1}) = \phi_M \left(\begin{bmatrix} \mathbf{x}_{T-1} \\ \mathbf{x}_T \end{bmatrix}; \begin{bmatrix} \widehat{\mathbb{E}} \mathbf{X}_T \\ \widehat{\mathbb{E}} [\mathcal{P}(\mathbf{X}_T)] \end{bmatrix}, \begin{bmatrix} \widehat{\text{Var}}_V \mathbf{X}_T & \widehat{\text{Cov}}(\mathbf{X}_T, \mathcal{P}(\mathbf{X}_T)) \\ \widehat{\text{Cov}}(\mathcal{P}(\mathbf{X}_T), \mathbf{X}_T) & \widehat{\text{Var}}_U \mathcal{P}(\mathbf{X}_T) \end{bmatrix} \right). \quad (66)$$

The marginal (54) is simply the truncation of the above.

It turns out that we never need to explicitly evaluate such a density, because of the following result:

Proposition 2. Partition $\mathbf{x} = \begin{bmatrix} \mathbf{x}_k \\ \mathbf{x}_\ell \end{bmatrix}$ so $X = \begin{bmatrix} X_k \\ X_\ell \end{bmatrix}$, and

$$X \sim \phi_M \left(\begin{bmatrix} \mathbf{x}_k \\ \mathbf{x}_\ell \end{bmatrix}; \begin{bmatrix} \bar{X}_k \\ \bar{X}_\ell \end{bmatrix}, \begin{bmatrix} \widehat{\text{Var}}_V X_k & \widehat{\text{Cov}}(X_\ell, X_k) \\ \widehat{\text{Cov}}(X_k, X_\ell) & \widehat{\text{Var}}_V(X_\ell) \end{bmatrix} \right). \quad (22)$$

In ensemble form, conditioning (9) becomes

$$X, \mathbf{x}_k^* \mapsto X_\ell + \widehat{\text{Cov}}(X_\ell, X_k) \widehat{\text{Var}}_V^{-1}(X_k) (\mathbf{x}_k^* \mathbf{B} - X_k) \quad (23)$$

The time cost of (23) is $\mathcal{O}(N^3 + N^2 D_{\mathbf{x}_k})$. Marginalisation (10) is simply truncation, $X \mapsto X_k$.

Proof. The equality (23) follows from 7 with the substitution of (22).

Notably we do not need to construct $\widehat{\text{Var}}_V(X_\ell)$, and can use Woodbury formula to efficiently solve the linear system involving $\widehat{\text{Var}}_V^{-1}(X_k)$. \square

We can use this to calculate an observation-conditional update, since

$$\begin{bmatrix} X_T \\ Y_T \end{bmatrix} \Big| \mathbf{y}_{1:T-1} = \begin{bmatrix} X_T | \mathbf{y}_{1:T-1} \\ \mathcal{H}(X_T | \mathbf{y}_{1:T-1}) \end{bmatrix}. \quad (67)$$

We can use (23) to calculate $X_T | \mathbf{y}_{1:T}$ by using \mathbf{y}_T as the observations \mathbf{x}_k^* in the update. We have thus obtained sampled from the filtered distribution without ever evaluating its density.

E. Matheron updates for Gaussian variates

The pathwise Gaussian process update (*Matheron update*), credited to Matheron by Wilson et al. (2021); Doucet (2010) is a method of simulating from a conditional of some jointly Gaussian variate. If

$$\begin{bmatrix} \mathbf{y} \\ \mathbf{w} \end{bmatrix} \sim \mathcal{N} \left(\begin{bmatrix} m_{\mathbf{y}} \\ m_{\mathbf{w}} \end{bmatrix}, \begin{bmatrix} K_{\mathbf{y}\mathbf{y}} & K_{\mathbf{y}\mathbf{w}} \\ K_{\mathbf{w}\mathbf{y}} & K_{\mathbf{w}\mathbf{w}} \end{bmatrix} \right) \quad (68)$$

then the moment of the \mathbf{w} -conditional distribution are

$$\mathbb{E}[\mathbf{y} | \mathbf{w}=\mathbf{w}^*] = m_{\mathbf{y}} + K_{\mathbf{w}\mathbf{y}} K_{\mathbf{w}\mathbf{w}}^{-1} (\mathbf{w}^* - m_{\mathbf{w}}) \quad \text{first moment} \quad (69)$$

$$\text{Var}[\mathbf{y} | \mathbf{w}=\mathbf{w}^*] = K_{\mathbf{y}\mathbf{y}} - K_{\mathbf{w}\mathbf{y}} K_{\mathbf{w}\mathbf{w}}^{-1} K_{\mathbf{y}\mathbf{w}}. \quad \text{second moment} \quad (70)$$

Proposition 7. For $\begin{bmatrix} \mathbf{y} \\ \mathbf{w} \end{bmatrix}$ as in (68), the variates in the following mapping

$$\mathbf{y}, \mathbf{w}, \mathbf{w}^* \mapsto \mathbf{y} + K_{\mathbf{w}\mathbf{y}} K_{\mathbf{w}\mathbf{w}}^{-1} (\mathbf{w}^* - \mathbf{w}) \quad (71)$$

satisfy the moment conditions (69) and (70) and thus $(\mathbf{y} + K_{\mathbf{w}\mathbf{y}} K_{\mathbf{w}\mathbf{w}}^{-1} (\mathbf{w}^* - \mathbf{w})) \stackrel{d}{=} (\mathbf{y} | \mathbf{w}=\mathbf{w}^*)$.

Proof. Taking moments of (71)

$$\begin{aligned} \mathbb{E}[\mathbf{y} + K_{\mathbf{w}\mathbf{y}} K_{\mathbf{w}\mathbf{w}}^{-1} (\mathbf{w}^* - \mathbf{w})] &= m_{\mathbf{y}} + K_{\mathbf{w}\mathbf{y}} K_{\mathbf{w}\mathbf{w}}^{-1} (\mathbf{w}^* - m_{\mathbf{w}}) \\ \text{Var}[\mathbf{y} + K_{\mathbf{w}\mathbf{y}} K_{\mathbf{w}\mathbf{w}}^{-1} (\mathbf{w}^* - \mathbf{w})] &= \text{Var}[\mathbf{y}] + \text{Var}[K_{\mathbf{w}\mathbf{y}} K_{\mathbf{w}\mathbf{w}}^{-1} (\mathbf{w}^* - \mathbf{w})] + \text{Cov}(\mathbf{y}, K_{\mathbf{w}\mathbf{y}} K_{\mathbf{w}\mathbf{w}}^{-1} (\mathbf{w}^* - \mathbf{w})) + \text{Cov}(K_{\mathbf{w}\mathbf{y}} K_{\mathbf{w}\mathbf{w}}^{-1} (\mathbf{w}^* - \mathbf{w}), \mathbf{y}) \\ &= K_{\mathbf{y}\mathbf{y}} + K_{\mathbf{w}\mathbf{y}} K_{\mathbf{w}\mathbf{w}}^{-1} K_{\mathbf{w}\mathbf{w}} K_{\mathbf{w}\mathbf{w}}^{-1} K_{\mathbf{y}\mathbf{w}} - 2K_{\mathbf{y}\mathbf{w}} K_{\mathbf{w}\mathbf{w}}^{-1} K_{\mathbf{w}\mathbf{y}} \\ &= K_{\mathbf{y}\mathbf{y}} - K_{\mathbf{w}\mathbf{y}} K_{\mathbf{w}\mathbf{w}}^{-1} K_{\mathbf{y}\mathbf{w}} \end{aligned}$$

we see that both first and second moment conditions are satisfied. \square

Note that this update does not require us to calculate $K_{\mathbf{y}\mathbf{y}}$ and further, may be conducted without needing to evaluate the density of the observation.

F. Nearly-low-rank matrices

Suppose the $K = V + kLL^\top$ where L is a $D \times N$ matrix, V is $D \times D$ and $V = \text{diag}(v)$ and $k \in \{-1, 1\}$ is the *sign* of the matrix. We are primarily interested in such matrices in the case that $N \ll D$, which case we have called *nearly-low-rank*, when their computational properties are favourable for our purposes. This is in contrast to matrices with no particular exploitable structure, which we refer to as *dense*.

Throughout this section we assume that the matrices in question are positive definite; and that all operations are between conformable operations. We refer to the matrix L as the *component* of the nearly-low-rank matrix, and the diagonal matrix V .

If $N \geq D$ the name is misleading since they are not truly *low-rank*; the identities we write here still hold, but are not computationally expedient.

F.1. Multiplication by a dense matrix

The matrix product of an arbitrary matrix with a nearly-low-rank matrix may be calculated efficiently by grouping operations, since $KX = VX \pm U(U^\top X)$, which has a time cost of $\mathcal{O}(ND^2)$ and which may be calculated without forming the full matrix K . The result is not in general also a nearly-low-rank matrix.

F.2. Addition

The matrix sum of two nearly-low-rank matrices with the same sign is also a nearly-low-rank matrix. Suppose $K = V + kLL^\top$, $K' = V' + kL'L'^\top$,

$$K + K' = V + V' + kLL^\top + kL'L'^\top \quad (72)$$

$$= V + V' + k \begin{bmatrix} L & L' \end{bmatrix} \begin{bmatrix} L & L' \end{bmatrix}^\top. \quad (73)$$

The new matrix, is also nearly low rank with has nugget term $V + V'$ and component $\begin{bmatrix} L & L' \end{bmatrix}$.

F.3. Cheap nearly-low-rank inverses

Inverses of nearly-low-rank matrices are once again nearly-low-rank matrices, and may be found efficiently.

Proposition 8. Choose nearly-low rank $K = V + LL^\top$, i.e. with sign k positive. Then its inverse

$$K^{-1} = V^{-1} - RR^\top \quad (74)$$

is also nearly-low-rank, of the same component dimension, but with a negative sign, with

$$R = V^{-1}L \text{ chol} \left((I + L^\top V^{-1}L)^{-1} \right). \quad (75)$$

where $\text{chol}(A)$ denotes a decomposition $\text{chol}(A)\text{chol}(A)^\top = A$.

Proof. Using the Woodbury identity,

$$\begin{aligned} K^{-1} &= V^{-1} - V^{-1}L(I + L^\top V^{-1}L)^{-1}L^\top V^{-1} \\ &= V^{-1} - RR^\top. \end{aligned}$$

□

Proposition 9. Choose nearly-low rank $P = U - RR^\top$, i.e. with sign k negative. Then its inverse

$$P^{-1} = U^{-1} - LL^\top \quad (76)$$

is also nearly-low-rank, of the same component dimension, but with a positive sign, with

$$L = U^{-1}R \text{ chol} \left((-I + R^\top U^{-1}R)^{-1} \right). \quad (77)$$

Proof. Using the Woodbury identity,

$$P^{-1} = U^{-1} - U^{-1}R(-I + R^T U^{-1}R)^{-1}R^T U^{-1} \quad (78)$$

$$= U^{-1} + LL^T \quad (79)$$

□

The cost of the inversion is the same for both, $\mathcal{O}(N^2D + N^3) = \mathcal{O}(N^3)$ for the construction of the Cholesky factor, and $\mathcal{O}(DN^2)$ for the requisite matrix multiplies. The space cost is $\mathcal{O}(ND)$.

For a given $K = V + kLL^T$, the term $(kI + L^T V^{-1}L)$ is referred to as the *capacitance* of the matrix by convention.

F.4. Exact inversion when the component is high-rank

Suppose $P = U - RR^T$ where the $D \times N$ components high rank, in the sense that $N > D$. Then the low rank inversion to calculate P^{-1} is no longer cheap, since the $\mathcal{O}(N^D)$ cost is greater than naive inversion of the dense matrix, at $\mathcal{O}(D^3)$. In this case, it is cheaper to recover a nearly-low-rank inverse by an alternate method. Note that $(U - P)^{-1} = U^{-1} - U^{-1}(U^{-1} - P^{-1})^{-1}U^{-1}$. We find the eigendecomposition

$$P^{-1} = U^{-1} + LL^T \quad (80)$$

for some L . Such an L is given by $L = Q\Lambda^{1/2}$ for $Q\Lambda Q^T = P^{-1} - U^{-1}$ a spectral decomposition. In the case that the diagonal U is constant this may be found more efficiently.

If, instead, we wish to invert $K = V + LL^T$ we need to find $(-V + K)^{-1} = -V^{-1} - V^{-1}(K^{-1} - V^{-1})^{-1}V^{-1}$, so we decompose instead $Q\Lambda Q = V^{-1}(K^{-1} - V^{-1})^{-1}V^{-1}$ and define $R = Q\Lambda^{-1/2}$. Then the nearly-low-rank form of the inverse is $-V^{-1} - RR^T$.

F.5. Reducing component rank

We use the SVD to efficiently reduce the rank of the components in the nearly-low-rank matrix in the sense of finding a Frobenius-distance-minimising approximation.

Suppose $K = V + LL^T$ where L is a $D \times M$ matrix, I is $D \times D$ and $V = \text{diag}(v)$. Let YSZ^T be the “thin” SVD of L , i.e. $Y \in \mathbb{R}^{D \times M}$, $S \in \mathbb{R}^{M \times M}$, $Z \in \mathbb{R}^{M \times M}$ with $Y^T Y = I_N$, $Z^T Z = I_N$, and S diagonal with non-negative entries. Then

$$LL^T = YSZ^T ZSY^T = YS^2 Y^T.$$

First we note that should any singular values in S be zero, we may remove the corresponding columns of Y and Z without changing the product, so their exclusion is exact. Next, we note that if we choose the largest S singular values of S , setting the rest to zero, we obtain a Frobenius approximation of LL^T of rank S .

An SVD that captures the top N singular values may be found by conventional thin SVD at a cost of $\mathcal{O}(DN^2)$.

G. Gaussians with nearly-low-rank parameters

We recall the forms of the Gaussian density introduced in section 2.2.3, in *moments* form using the mean \mathbf{m} and covariance matrix K ,

$$\mathbf{x} \sim \mathcal{N}(\mathbf{m}, K) = \mathcal{N}(\mathbb{E}[\mathbf{x}], \text{Var}(\mathbf{x})).$$

and the *canonical* form,

$$\mathbf{x} \sim \mathcal{N}_C(\mathbf{n}, P) = \mathcal{N}_C(\text{Var}^{-1}(\mathbf{x})\mathbb{E}[\mathbf{x}], \text{Var}^{-1}(\mathbf{x})).$$

which uses the information vector \mathbf{n} and the *precision matrix*, P with $\mathbf{n} = K^{-1}\mathbf{m}$, $P = K^{-1}$. The (equivalent) densities induced by these parameterisations are

$$f(\mathbf{x}) \propto \frac{1}{2}(\mathbf{x} - \mathbf{m})^T K^{-1}(\mathbf{x} - \mathbf{m}) = \frac{1}{2}\mathbf{x}^T P\mathbf{x} - \mathbf{n}^T \mathbf{x}$$

We associate a given Gaussian ensemble with a moments-form Gaussian in the natural way,

$$X_{\sigma^2} \sim \mathcal{N}(\mathbf{m}, \mathbf{K}) = \mathcal{N}(\widehat{\mathbb{E}}[X], \widehat{\text{Var}}_{\sigma^2}(X))$$

introducing a parameter σ^2 which we use to ensure invertibility of the covariance if needed.

We associate with each moments-form Gaussian a *canonical form* which may be cheaply calculated by using the by using the low-rank representation of the covariance prop 8,

$$\begin{aligned} X_{\sigma^2} &\sim \mathcal{N}(\mathbf{m}, \mathbf{K}) \\ \mathbf{m} &= \widehat{\mathbb{E}}(X) = \bar{X} \\ \mathbf{K} &= \widehat{\text{Var}}_{\sigma^2}(X) = \sigma^2 + \check{X}\check{X}^\top \\ &\Leftrightarrow \\ X_{\sigma^2} &\sim \mathcal{N}_C(\mathbf{n}, \mathbf{P}) \\ \mathbf{n} &= \widehat{\text{Var}}_{\sigma^2}^{-1}(X)\widehat{\mathbb{E}}(X) = \mathbf{P}\bar{X} \\ \mathbf{P} &= \widehat{\text{Var}}_{\sigma^2}^{-1}(X) = \sigma^{-2}\mathbf{I} - \mathbf{R}\mathbf{R}^\top. \end{aligned}$$

where we introduced $\mathbf{R} = \check{X} \text{chol} \left(\left(\mathbf{I} + \sigma^{-2}\check{X}^\top\check{X} \right)^{-1} \right)$.

We may recover \mathbf{m} and \mathbf{K} from \mathbf{n} and \mathbf{P} by

$$\begin{aligned} \mathbf{K} &= \mathbf{P}^{-1} \\ \mathbf{m} &= \mathbf{P}^{-1}\mathbf{n}. \end{aligned}$$

this time using the alternative low rank inverse formula 9.

H. Ensemble recovery

Suppose that after belief propagation we update our belief about a given query variable node to $b(\mathbf{x}_{\mathcal{Q}}) \sim \mathcal{N}_M(\mathbf{x}_{\mathcal{Q}}; \mathbf{m}, \mathbf{K}_{\mathcal{Q}})$. In the Ensemble message passing setting we have nearly-low-rank $\mathbf{K}_{\mathcal{Q}} = \mathbf{V}_{\mathcal{Q}} + \mathbf{L}_{\mathcal{Q}}\mathbf{L}_{\mathcal{Q}}^\top$. In order to convert this belief into ensemble samples, we choose the transformation T which maps prior ensemble $X_{\mathcal{Q}}$ from the previous iterate to an updated ensemble $X'_{\mathcal{Q}} = T(X_{\mathcal{Q}})$ such that the (empirical) ensemble distribution is as similar as possible, in some metric d to $\mathcal{N}_M(\mathbf{x}_{\mathcal{Q}}; \mathbf{m}, \mathbf{K}_{\mathcal{Q}})$. Hereafter we suppress the subscript Q for compactness, and because what follows is generic for ensemble moment matching. This amounts to choosing

$$T = \operatorname{argmin}_{T^*} d(\mathcal{N}_M(\cdot; \widehat{\mathbb{E}}T(X), \widehat{\text{Var}}_{\sigma^2}T(X)), \mathcal{N}_M(\cdot; \mathbf{m}, \mathbf{K})), \quad (81)$$

We wish to do this *without forming* $\mathbf{K} \in \mathbb{R}^{D \times D}$, which may be prohibitively memory expensive, by exploiting its nearly-low-rank decomposition. We restrict ourselves to the family of affine transformations $T_{\boldsymbol{\mu}, \mathbf{T}} : X \mapsto \boldsymbol{\mu} + \check{X}\mathbf{T}$ where the parameters $\boldsymbol{\mu} \in \mathbb{R}^D$, $\mathbf{T} \in \mathbb{R}^{N \times N}$ must be chosen. If we minimise between the belief and ensemble distributions empirical covariances, the solution is

$$\boldsymbol{\mu} = \widehat{\mathbb{E}}X \quad (82)$$

$$\mathbf{T} = \operatorname{argmin}_{\mathbf{T}} \left\| \widehat{\text{Var}}_{\sigma^2}(\check{X}\mathbf{T}) - \mathbf{K} \right\|_F^2 \quad (83)$$

$$= \operatorname{argmin}_{\mathbf{T}} \left\| \widehat{\text{Var}}_{\sigma^2}(T(X)) - \mathbf{L}\mathbf{L}^\top - \mathbf{V} \right\|_F^2 \quad (84)$$

$$= \operatorname{argmin}_{\mathbf{T}} \left\| \frac{\check{X}\mathbf{T}\mathbf{T}^\top\check{X}^\top}{N-1} - \mathbf{V}_{-\sigma^2} - \mathbf{L}\mathbf{L}^\top \right\|_F^2, \quad (85)$$

Here we have introduced $\mathbf{V}_{-\sigma^2} := \mathbf{V} - \sigma^2\mathbf{I}$. Note that minimisers of L with respect to \mathbf{T} are not unique, because L depends only on $\mathbf{T}\mathbf{T}^\top$. For example, we may take any orthogonal transformation \mathbf{U} of \mathbf{T} and obtain the same $(\mathbf{T}\mathbf{U})(\mathbf{T}\mathbf{U})^\top =$

$\mathbb{T}\mathbb{U}\mathbb{U}^\top\mathbb{T}^\top = \mathbb{T}\mathbb{T}^\top$. We instead optimise $\mathbb{M} = \mathbb{T}\mathbb{T}^\top$ over the space of $N \times N$ PSD matrices $\mathbb{M}_+^N = \{\mathbb{M} \in \mathbb{R}^{N \times N} \mid \mathbb{M} = \mathbb{M}^\top, \mathbb{M} \succeq 0\}$. That is, we consider the problem

$$\mathbb{M}^* = \operatorname{argmin}_{\mathbb{M} \in \mathbb{M}_+^N} L(\mathbb{M}) \quad (86)$$

where

$$L(\mathbb{M}) := \operatorname{argmin}_{\mathbb{M}} \left\| \frac{1}{N-1} \check{\mathbb{X}}\mathbb{M}\check{\mathbb{X}}^\top - \mathbb{L}\mathbb{L}^\top - \mathbb{V}_{-\sigma^2} \right\|_F^2. \quad (87)$$

This is a convex problem in \mathbb{M} . The derivatives are given by (Laue et al., 2018; 2020)

$$\begin{aligned} \nabla_{\mathbb{M}} L &= \frac{2}{N-1} \check{\mathbb{X}}^\top \left(\frac{\check{\mathbb{X}}\mathbb{M}\check{\mathbb{X}}^\top}{N-1} - \mathbb{L}\mathbb{L}^\top - \mathbb{V}_{-\sigma^2} \right) \check{\mathbb{X}} \\ &= \frac{2}{N-1} \left(\frac{\check{\mathbb{X}}^\top \check{\mathbb{X}}\mathbb{M}\check{\mathbb{X}}^\top \check{\mathbb{X}}}{N-1} - (\check{\mathbb{X}}^\top \mathbb{L})(\check{\mathbb{X}}^\top \mathbb{L})^\top - \check{\mathbb{X}}^\top \mathbb{V}_{-\sigma^2} \check{\mathbb{X}} \right) \end{aligned}$$

An unconstrained solution in \mathbb{M}' may be found by setting the gradient to zero,

$$\check{\mathbb{X}}^\top \check{\mathbb{X}}\mathbb{M}'\check{\mathbb{X}}^\top \check{\mathbb{X}} = (N-1) \left(\check{\mathbb{X}}^\top \mathbb{L}(\check{\mathbb{X}}^\top \mathbb{L})^\top + \check{\mathbb{X}}^\top \mathbb{V}_{-\sigma^2} \check{\mathbb{X}} \right).$$

This linear system may be solved at $\mathcal{O}(N^3)$ cost for the ensemble size N . As $\check{\mathbb{X}}^\top \check{\mathbb{X}}$ is Hermitian we also economise by using specialised methods such as pivoted LDL decomposition. Using the same decomposition we also find the required $\mathbb{M}^* = \mathbb{T}\mathbb{T}^\top$, choosing $\mathbb{T} = \mathbb{U}(S^+)^{1/2}$. By careful ordering of operations we may calculate the RHS with cost $\mathcal{O}(DM^2)$ for a total cost of $\mathcal{O}(N^3 + DN^2 + DM^2)$.

I. Computational costs

We summarise results from Ortiz et al. (2021) and sections 3.2 and 3.4 in Table 2. Note that GEnBP is never worse than linear in D , unlike GaBP. On the other hand, GaBP does not depend upon node degree K or ensemble size N .

Table 2: Computational Costs for Gaussian Belief Propagation and Ensemble Belief propagation for node dimension D , node degree K , ensemble size N . For simplicity, all variables are assumed to have the same dimension.

Operation		GaBP	GEnBP
Time Complexity	Simulation	$\mathcal{O}(1)$	$\mathcal{O}(N)$
	Error propagation	$\mathcal{O}(D^3)$	—
	Jacobian calculation	$\mathcal{O}(D)$	—
	Covariance matrix	$\mathcal{O}(D^2)$	$\mathcal{O}(N+D)$
	Factor-to-node message	$\mathcal{O}(D^3)$	$\mathcal{O}(K^3N^3 + DN^2K^2)$
	Node-to-factor message	$\mathcal{O}(D^2)$	$\mathcal{O}(1)$
	Ensemble recovery	—	$\mathcal{O}(K^3N^3 + DN^2K^2)$
Canonical-Moments form conversion	$\mathcal{O}(D^3)$	$\mathcal{O}(N^3 + N^2D)$	
Space Complexity	Covariance Matrix	$\mathcal{O}(D^2)$	$\mathcal{O}(ND)$
	Precision Matrix	$\mathcal{O}(D^2)$	$\mathcal{O}(ND)$

J. Alternative linearisations and low rank decompositions

In response to a reviewer question, we investigate whether GEnBP is “just” a low-rank decomposition of the GaBP algorithm. We argue that it is not. Rather the relationship is that diagrammed by Fig. 10. Although the GEnBP and GaBP algorithms both use Gaussian approximations, they do not use the same Gaussian approximations. This is why we observe in Sec. 4 that GEnBP is able to surpass GaBP in accuracy and not just speed. We noted in app. C.3 that GaBP include not only a choice of Gaussian density family, which it shares with GEnBP, but also a particular means of approximating nonlinear factors which it does not. That apparently minor difference has large implications. We expand upon some of the differences and implications in this section.

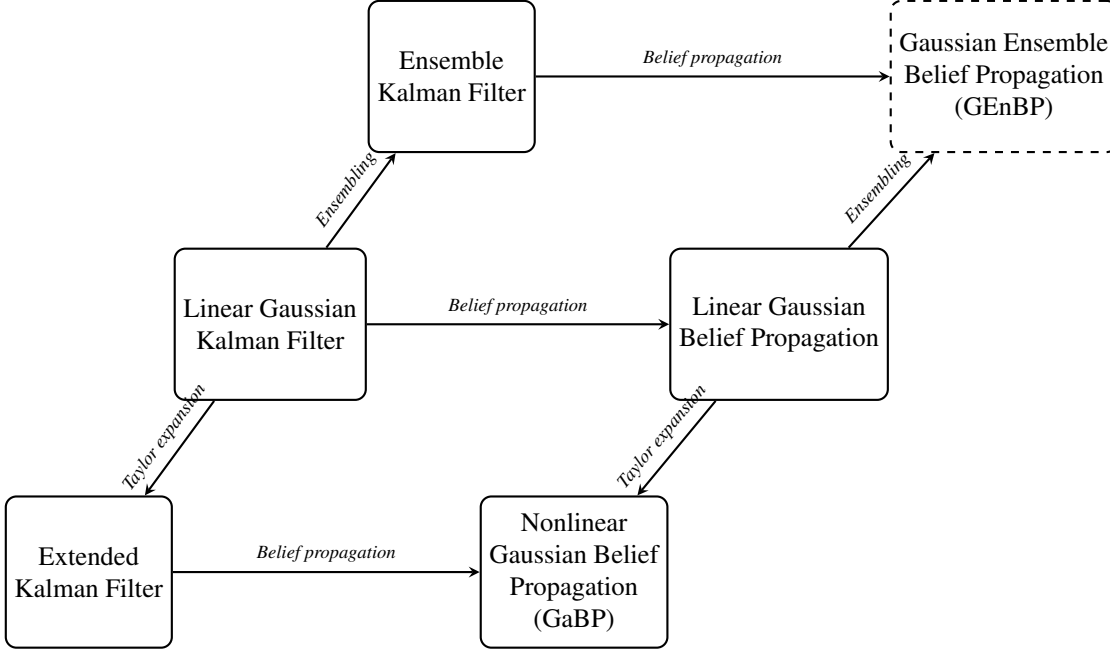


Figure 10: Relationship between GEnBP and GaBP.

Consider how the joint density of a factor $\mathbf{x}_2 = \mathcal{P}(\mathbf{x}_1)$ to make the differences explicit. For the sake of simplicity, suppose $D_1 = D_2 = D$. Two alternatives for covariance estimation have been discussed in this work: GaBP uses propagation of errors,

$$\text{Var} \begin{bmatrix} \mathbf{x}_1 \\ \mathbf{x}_2 \end{bmatrix} \simeq \begin{bmatrix} \text{Var} \mathbf{x}_1 & J(\mathbf{m}_1) \text{Var} \mathbf{x}_1 \\ \text{Var} \mathbf{x}_1 J(\mathbf{m}_1)^\top & J(\mathbf{m}_1) \text{Var} \mathbf{x}_1 J^\top(\mathbf{m}_1) \end{bmatrix} \quad (88)$$

where $J(x)$ is the jacobian matrix of \mathcal{P} at x . GEnBP, by contrast, uses the empirical estimate

$$\text{Var} \begin{bmatrix} \mathbf{x}_1 \\ \mathbf{x}_2 \end{bmatrix} \simeq \widehat{\text{Var}}_{\sigma^2 \mathbf{I}} \begin{bmatrix} x^{(1)} & \dots & x^{(N)} \\ \mathcal{P}(x^{(1)}) & \dots & \mathcal{P}(x^{(N)}) \end{bmatrix}. \quad (89)$$

As noted in App. I, the costs of (89) is greater than (88) both in time and space. There are two components to this cost:

Firstly, the cost of generating the ensemble (in GenBP) and the jacobians (in GaBP). In GEnBP, we need to generate N samples from the prior distribution, so the cost here scales as N in general. The cost of calculating the Jacobian for the GaBP depends on the function but in general is $\mathcal{O}(D)$.

Secondly, taking the matrix products in each of these covariance matrices. The matrix multiplication in (88) is $\mathcal{O}(D^3)$, since it involved the product of three $D \times D$ matrices. The empirical covariance calculation in (89) is $\mathcal{O}(DN)$. We note that it *would* be $\mathcal{O}(D^2N)$ if we were to calculate the full covariance matrix in GEnBP, but the central lesson of this paper is that we never need to calculate that product, and it suffices to calculate the deviance matrices.

It seems that at this stage, GEnBP dominates when $N < D$. We note that in the subsequent belief propagation the story is more complicated but that GEnBP has generally cheaper belief propagation steps (except where node degree is high). We might ask if GaBP can also benefit from these low-rank belief updates.

Suppose we wished to construct a 3rd option, a *low rank GaBP* (LRGaBP) which used a low-rank decomposition of the covariance matrix to conduct approximate GaBP. First, we would find rank N decomposition of the prior covariance $\text{Var} \mathbf{x}_1 \approx LL^\top$, with $L \in \mathbb{R}^{D \times N}$, say by eigendecomposition, which is naively a D^3 operation, or $\mathcal{O}(D^2 \log N + N^2 D + N^3)$

by the method of (Halko et al., 2010, 6.1). Then the joint variance arising from propagation-of-errors is

$$\text{Var} \begin{bmatrix} \mathbf{x}_1 \\ \mathbf{x}_2 \end{bmatrix} \simeq \begin{bmatrix} \text{Var} \mathbf{x}_1 & J(\mathbf{m}_1) \text{Var} \mathbf{x}_1 \\ \text{Var} \mathbf{x}_1 J(\mathbf{m}_1)^\top & J(\mathbf{m}_1) \text{Var} \mathbf{x}_1 J^\top(\mathbf{m}_1) \end{bmatrix} \quad (90)$$

$$= \begin{bmatrix} \text{LL}^\top & J(\mathbf{m}_1)\text{LL}^\top \\ \text{LL}^\top J(\mathbf{m}_1)^\top & J(\mathbf{m}_1)\text{LL}^\top J^\top(\mathbf{m}_1) \end{bmatrix} \quad (91)$$

$$= \begin{bmatrix} \text{L} \\ J(\mathbf{m}_1)\text{L} \end{bmatrix} \begin{bmatrix} \text{L} \\ J(\mathbf{m}_1)\text{L} \end{bmatrix}^\top \quad (92)$$

This is indeed a low-rank decomposition, amenable to similar tricks as the other low-rank tricks outlined in app. F. However, it is not computationally competitive. J is $D \times D$ so the product costs $\mathcal{O}(D^2N)$, plus the $\mathcal{O}(D)$ cost of calculating the Jacobian. We summarise the costs of this hypothetical LRGaBP step in table 3. Notably, while the precise relationship between the algorithms depends upon the exact problem structure, we should generally expect GEnBP to be more efficient than LRGaBP for high dimensional problems for a fixed N , since GEnBP is never worse than LRGaBP, and in many cases has a lower exponent in D .

Further, since LRGaBP is an approximation to GaBP, the accuracy of LRGaBP to be bounded above by the accuracy of GaBP. GEnBP, as a different approximation to the target estimand, has no such restriction.

Table 3: Computational Costs for Gaussian Belief Propagation, Ensemble Belief propagation, and the hypothetical Low Rank Gaussian Belief Propagation for node dimension D , ensemble size/component rank N .

Operation		GaBP	GEnBP	LRGaBP
Time Complexity	Simulation	$\mathcal{O}(1)$	$\mathcal{O}(N)$	$\mathcal{O}(1)$
	Error propagation	$\mathcal{O}(D^3)$	—	$\mathcal{O}(D^2N)$
	Jacobian calculation	$\mathcal{O}(D)$	—	$\mathcal{O}(D)$
	Covariance SVD	—	$\mathcal{O}(N^3 + N^2D)$	$\mathcal{O}(D^2 \log N + N^3 + N^2D)$
Space Complexity	Covariance Matrix	$\mathcal{O}(D^2)$	$\mathcal{O}(ND)$	$\mathcal{O}(ND + D^3)$
	Precision Matrix	$\mathcal{O}(D^2)$	$\mathcal{O}(ND)$	$\mathcal{O}(ND)$